Physica D 422 (2021) 132903

Contents lists available at ScienceDirect

Physica D

journal homepage: www.elsevier.com/locate/physd

Epidemic models with discrete state structures☆

Suli Liu [a,*], Michael Y. Li [b]

[a] School of Mathematics, Jilin University, Changchun, Jilin Province, 130012, China
[b] Department of Mathematical and Statistical Sciences, University of Alberta, Edmonton, AB, T6G 2G1, Canada

ARTICLE INFO

Article history:
Received 11 May 2020
Received in revised form 7 March 2021
Accepted 9 March 2021
Available online 24 March 2021
Communicated by V.M. Perez-Garcia

Keywords:
Epidemic models
State of infections
State structures
Basic reproduction number
COVID-19 pandemic
Global stability

ABSTRACT

The state of an infectious disease can represent the degree of infectivity of infected individuals, or susceptibility of susceptible individuals, or immunity of recovered individuals, or a combination of these measures. When the disease progression is long such as for HIV, individuals often experience switches among different states. We derive an epidemic model in which infected individuals have a discrete set of states of infectivity and can switch among different states. The model also incorporates a general incidence form in which new infections are distributed among different disease states. We discuss the importance of the transmission–transfer network for infectious diseases. Under the assumption that the transmission–transfer network is strongly connected, we establish that the basic reproduction number $\mathcal{R}_0$ is a sharp threshold parameter: if $\mathcal{R}_0 \leq 1$, the disease-free equilibrium is globally asymptotically stable and the disease always dies out; if $\mathcal{R}_0 > 1$, the disease-free equilibrium is unstable, the system is uniformly persistent and initial outbreaks lead to persistent disease infection. For a restricted class of incidence functions, we prove that there is a unique endemic equilibrium and it is globally asymptotically stable when $\mathcal{R}_0 > 1$. Furthermore, we discuss the impact of different state structures on $\mathcal{R}_0$, on the distribution of the disease states at the unique endemic equilibrium, and on disease control and preventions. Implications to the COVID-19 pandemic are also discussed.

1. Introduction

Many infectious diseases have a long course of progression in infected hosts, often through several distinct stages. These include viral infections such as HIV and viral Hepatitis, bacterial diseases such as Tuberculosis and Cholera, parasitic diseases such as Malaria and Schistosomiasis. Infected individual hosts many experience changes in levels of pathogen load, which impacts the individual's infectivity, and levels of antibodies and immune cells, which impact host immunity, either due to the natural disease progression or through medical interventions. Individual variations of these important factors are key sources of heterogeneity in the host population, and can be essential for understanding the dynamical complexity of the disease transmission and spread.

For an infectious disease, we consider the *state* of an individual host that represents all or a subset of important epidemiological, immunological, and ecological factors for disease progression and transmission. In the case of HIV-1 infection, an individual host's state of infection can be simply represented by a vector-valued variable $(s_1, s_2) \in \mathbb{R}^2_+$, where s_1 in the level of HIV-1 viral load and s_2 the level of CD4 count, common measures used to gauge the HIV-1 progression of a patient. The values of s_i can vary over time as the infection progresses and when the antiretroviral treatments (ART) are given, and they typically exhibit a high degree of individual variations.

The concept of state of infection of an individual host was used in the classical paper of Kermack and McKendric [1], and has since been explored in mathematical models under different terms. In staged progression models of HIV, an infected individual can progress forward through different stages or backward due to treatment [2–12]. The stages of disease progression is a good example of the state of an infected individual. The concept of state of infection is, however, more general than that of stages and can unify many different approaches to model disease heterogeneity. For instance, the concept of state or substate can be applied to susceptible hosts to represent different level of host susceptibility to infection or reinfection after recovery. Such a consideration will lead to the investigation of the impact of differential susceptibility on disease transmission (see [4]). The concept of state or substate can also be considered for vaccinated or immune hosts and used to measure individual variations as well as community distributions of level of antibodies and immunity. The

☆ This work was done during a visit of SL to the University of Alberta supported by the China Scholarship Council (CSC), and partly supported by Jilin Province education department of China (JJKH20211033KJ). Research of MYL is supported in part by Natural Sciences and Engineering Council of Canada (NSERC) and Canada Foundation for Innovation (CFI).
* Corresponding author.
E-mail addresses: liusl15@mails.jlu.edu.cn (S. Liu), mli@math.ualberta.ca (M.Y. Li).

https://doi.org/10.1016/j.physd.2021.132903
0167-2789/

concept of state can also be extended to individual characteristics including spatial location, chronological age, development stage, size etc [13]. And the distributions of individual characteristics directly influence the dynamics of population which could be generated as the state space of measures [14–16]. Interpretation of the traditional epidemic models in a state-space framework was used to track the evolution of Flu in the United States [17] and predict intervention effect for COVID-19 in Japan [18].

The concept of state has also been widely employed to diffusion models in the social and life sciences. For example, the Bass model for diffusion of innovation [19] and its generalizations and variations [20,21], models for the diffusion of information on social media [22], models for the spread of opinions [23], and models for the spread of innovations and transient fads [24]. Further information on this type of models can be found in more recent references (e.g. [25–27]).

Recent HIV research on nonprogressors and elite controllers [28,29], HIV-1 patients who can keep the HIV-1 progression under check without anti-retroviral treatment, suggests that to fully understand the progression of HIV-1 infection, we need to include in the disease state indicators of the immune system such as counts of HIV-1 specific cytotoxic T lymphocytes (CTLs), levels of anti-HIV-1 antibodies, as well as measures of anti-HIV-1 cytokines and other biomarkers in modelling studies. From a transmission viewpoint, the disease state should also include an individual's sexual preferences and a scoring of risky behaviours. This approach can stimulate a more comprehensive approach to modelling and better inform the prevention and control measures of the HIV epidemic (see e.g. [30,31]).

The transmission dynamics of the SARS-CoV-2 virus, which is responsible for the current COVID-19 pandemic, provided another good example of the importance of the state structure for epidemics. The significant number of asymptomatic infections is believed to be a key reason why the COVID-19 epidemics have proven to be more difficult to control than the SARS epidemics in 2003 [32,33]. The substate of asymptomatic infections can be studied in state-structured models. The current vaccines for COVID-19 are known to be highly effective to protect against serious symptoms and diseases, but their efficacy against transmission is still largely unknown [34]. While the vaccines can prevent serious diseases and deaths among seniors and people with underlying health, the vaccination of younger population may produce more asymptomatic disease carriers, whose existence was already known for COVID-19 even before the vaccines were available [33], if the efficacy of the vaccines against transmission is not sufficiently high. The impact of subgroup of asymptomatic carriers has been studied in the literature (e.g. [35]) and more recently for COVID-19 in the class of A-SIR models [36,37]. Other subgroups that capture the many characteristics of the COVID-19 were also considered in recent COVID-19 modelling, including undetected infections, infected but not infectious (latent), quarantined or isolated individuals, and hospitalized individuals (see e.g. [36,38,39] and references therein). Subgroups of infected individuals are special cases of the infection state and can be investigated under the framework of state-structures.

In our paper, we restrict our consideration to the state of infection among infected individuals and allow infected individuals switch their state of infection among finitely many different substates, hence creating a finite discrete state-structure. We formulate and investigate a class of epidemic models with a discrete state structure among infected individuals. Switch among different sub-states is given by a state-transfer matrix, which helps to capture the heterogeneity among the substates. We note that sub-state structures given by different state-transfer matrices may alter the probability distribution of the duration of infectiousness, and we refer the reader to the approach of the linear chain trick and its generalizations (see e.g. [40]) for this linkage. For modelling dynamical processes on networks, we refer the reader to the approximation frameworks of binary-state dynamical processes on networks [41] and its generalization [42].

In addition to carrying out a standard stability analysis of a relatively comprehensive model, the consideration of state has inspired us to investigate a new set of questions and problems that are of both biological and mathematical interests: (1) the impacts of state structures on the basic reproduction number $\mathcal{R}_0$; (2) the influence of different disease interventions on the population distribution among different disease states; and (3) global stability analysis is of a considerable mathematical challenge for the state-structure models, and the graph-theoretic approach to the construction of Lyapunov functions [43,44] was further improved and adapted for the proof of global stability.

Results in our paper include as special cases earlier results on multi-staged epidemic models (see e.g. [9] and reference therein). A continuous approach to modelling the state structure was considered in [45], and the resulting model is a system of differential–integral equations with nonlocal effects. In our model (2.1) with a discrete state structure in Section 2, mathematical results on global stability are obtained under more relaxed conditions than those for infinite dimensional systems as in [45].

The paper is organized as follows. We formulate our model in the next section. In Section 3, we derive the basic reproduction number and give its biological interpretations. In Section 4, we carry out mathematical analysis of the global dynamics of the model for the case $f(N) \equiv 1$: the disease free equilibrium P_0 is globally asymptotically stable when $\mathcal{R}_0 \leq 1$; and a unique endemic equilibrium P^* exists and is globally asymptotically stable when $\mathcal{R}_0 > 1$. In Section 5, we carry out numerical investigations of the impacts of the state structure on disease dynamics and outcomes.

2. Model formulation

We assume that the state of an infected individual is a finite set with a scalar index i, $i = 1, 2, \ldots, n$. For $1 \leq i \leq n$, let $I_i(t)$ denote the number of the infected individuals who are in the ith state at time t. Let $S(t)$ denote the number of susceptible individuals at time t, and $R(t)$ denote the number of removed individuals at time t. Here, an individual is considered removed if the individual no longer participates in the transmission process. This can happen if an individual is in the terminal illness, such as having AIDS in the case of HIV infection, or the individual is permanently immune from reinfection, as in the case of Measles, or individuals who are tested positive for the infection and isolated or hospitalized as in an COVID-19 epidemic. We use $N(t) = S(t) + I_1(t) + I_2(t) + \cdots + I_n(t)$ to represent the total number of individuals who are active in the infection process.

In the absence of the disease, we assume that the dynamics of population are described by a nonlinear differential equation: $S' = \theta(S)$, where $\theta(S)$ is a growth function with a carrying capacity. Common forms of $\theta(S)$ are $\theta(S) = \Lambda - dS$ (see [6,46,47]) and $\theta(S) = \Lambda + rS(1 - \frac{S}{K}) - dS$ (see [9,48]). We also assume that the disease transmission is horizontal and has a general nonlinear incidence function $f(N)\sum_{j=1}^{n} g_j(S, I_j)$, where $f(N)$ denotes the density dependence. Out of the total new infection $f(N)\sum_{j=1}^{n} g_j(S, I_j)$, we assume that a fraction $\alpha_i \geq 0$ will enter the ith state, and $\sum_{i=1}^{n} \alpha_i = 1$. Let $\zeta_i(I_i)$ denote the removal rate from I_i, which may include natural death, disease-caused death, and out-migration. A common form of ζ_i is the exponential removal $\zeta_i(I_i) = d_i I_i$. To describe the switches among different states, for given $1 \leq i, j \leq n$, let ϕ_{ij} denote the transfer rate from the jth state to the ith state, and by convention, $\phi_{ii} = 0$. For $1 \leq i \leq n$, the transfer rate from the ith state to the removed compartment

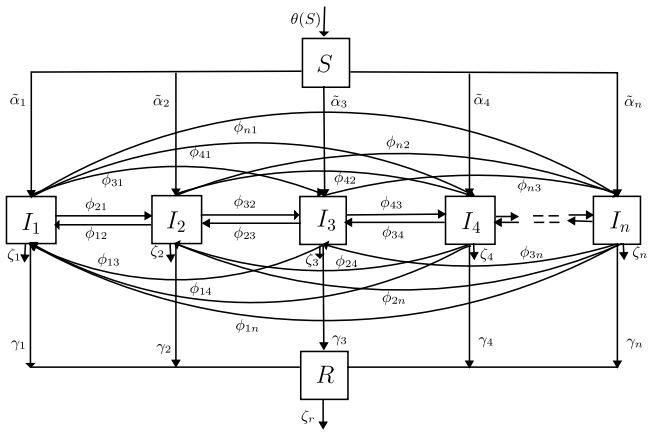

Fig. 1. The transfer diagram of model (2.1). Here the incidence terms are given by $\tilde{\alpha}_i = \alpha_i f(N)\sum_{j=1}^{n} g_j(S, I_j)$.

R is given by $\gamma_i(I_i)$. The removal rate from the compartment R is given by $\zeta_r(R)$. The preceding assumptions are illustrated in the transfer diagram in Fig. 1.

Based on these assumptions and using the transfer diagram, we derive an epidemic model with a discrete state structure described by the following system of nonlinear differential equations:

$$\begin{aligned} S' &= \theta(S) - f(N)\sum_{j=1}^{n} g_j(S, I_j),\\ I_i' &= \alpha_i f(N)\sum_{j=1}^{n} g_j(S, I_j) + \sum_{j=1}^{n}\phi_{ij}(I_j) - \sum_{j=1}^{n}\phi_{ji}(I_i) - \gamma_i(I_i) - \zeta_i(I_i),\\ &\quad i = 1, 2, \ldots, n. \end{aligned} \tag{2.1}$$

Since the removed population is no longer part of the transmission process and the variable R does not appear in the equations of S and I_i, we consider the following equation for the removed population R separately:

$$R' = \sum_{i=1}^{n}\gamma_i(I_i) - \zeta_r(R).$$

The general functions in model (2.1), $f(N)$, $g_j(S, I_j)$, $\phi_{ij}(I_j)$, $\gamma_i(I_i)$ and $\zeta_i(I_i)$ are assumed to be sufficiently smooth such that existence and uniqueness of solutions are satisfied. We further make the following biologically motivated assumptions:

- (H_1) There exists $\bar{S} > 0$ such that $\theta(\bar{S}) = 0$ and $\theta(S)(S - \bar{S}) < 0$, $\forall S \geq 0$, $S \neq \bar{S}$;
- (H_2) $f(N) : \mathbb{R}_+ \to \mathbb{R}_+$ is a nonincreasing positive function;
- (H_3) For $1 \leq j \leq n$, $g_j(S, I_j) \geq 0$ for all S, $I_j \geq 0$; and if $g_j \not\equiv 0$ then $g_j(S, I_j) = 0$ iff $S = 0$ or $I_j = 0$;
- (H_4) For $1 \leq i, j \leq n$, $\phi_{ji}(I_i) \geq 0$ for $I_i \geq 0$, $\phi_{ii}(I_i) \equiv 0$, and $\sum_{j=1}^{n}\phi_{ji}(I_i) = 0$ iff $I_i = 0$;
- (H_5) For $1 \leq i \leq n$, $\gamma_i(I_i) \geq 0$ for all $I_i \geq 0$ and $\gamma_i(0) = 0$;
- (H_6) For $1 \leq i \leq n$, $\zeta_i(0) = 0$, and there exists $d_i > 0$ such that $\zeta_i(I_i) \geq d_i I_i$ for all $I_i \geq 0$;
- (H_7) There exist constants $c_i \geq 0$, $\max_{1\leq i\leq n}\{c_i\} > 0$, such that $\lim_{I_i\to 0^+}\frac{g_i(\bar{S}, I_i)}{I_i} = c_i$;
- (H_8) There exist constants $0 \leq b_{ij} < \infty$, $1 \leq i, j \leq n$, $i \neq j$ such that $\lim_{I_j\to 0^+}\frac{\phi_{ij}(I_j)}{I_j} = b_{ij}$;
- (H_9) There exist constants $0 < a_i < \infty$, $1 \leq i \leq n$, $\lim_{I_i\to 0^+}\frac{\gamma_i(I_i)+\zeta_i(I_i)}{I_i} = a_i$.

It can be verified by examining direction of the vector fields on the boundary of $\mathbb{R}_+^{n+1}$ that solutions to system (2.1) with nonnegative initial conditions remain nonnegative for $t \geq 0$ and that the model is well defined. From the first equation of system (2.1) and assumptions (H_2), (H_3), we know that $S' \leq \theta(S)$. Assumption (H_1) implies that $\limsup_{t\to\infty} S(t) \leq \bar{S}$, a carrying capacity of the disease-free population. Adding all equations of (2.1) yields that

$$(S+I_1+I_2+\cdots+I_n)' = \theta(S) - \sum_{i=1}^{n}\gamma_i(I_i) - \sum_{i=1}^{n}\zeta_i(I_i) \leq \theta(S) - \sum_{i=1}^{n}\zeta_i(I_i).$$

By assumption (H_6), we have

$$(S + I_1 + I_2 + \cdots + I_n)' \leq \theta(S) - \sum_{i=1}^{n} d_i I_i.$$

Let $d^* = \min_{1\leq i\leq n}\{d_i\}$ and we assume that $d^* > 0$. Then

$$\begin{aligned} (S + I_1 + I_2 + \cdots + I_n)' &\leq \theta(S) + d^*S - d^*(S + I_1 + I_2 + \cdots + I_n)\\ &\leq M - d^*(S + I_1 + I_2 + \cdots + I_n), \end{aligned}$$

where $M \geq \max_{S\geq 0}\{\theta(S) + d^*S\}$, which implies

$$\limsup_{t\to\infty}(S + I_1 + I_2 + \cdots + I_n) \leq \tfrac{M}{d^*}.$$

Therefore, omega limit sets of system (2.1) are contained in the following bounded region:

$$\Gamma = \{(S, I_1, I_2, \ldots, I_n) \in \mathbb{R}_+^{n+1} \mid S \leq \bar{S}, S + I_1 + I_2 + \cdots + I_n \leq \tfrac{M}{d^*}\}. \tag{2.2}$$

It can be verified that Γ is positively invariant with respect to (2.1).

The function $f(N)$ in model (2.1) represents density dependence in the disease incidence. The monotonicity assumption on $f(N)$ in (H_2) is satisfied by the class $f(N) = 1/N^p$, $p \geq 0$, used in the literature. It is however a simplifying assumption. When $f(N)$ is non-monotone, it was shown in [49] using a simple SIR model that complex dynamics such as backward bifurcations and Hopf bifurcations can occur. Assumption (H_3) on the incidence function $g_j(S, I_j)$ allows many possibilities for disease transmission at different state. For instance, transmission coefficients can be 0 at states where the infected individual is latent or quarantined, and transmission coefficients can be substantially lower at a state where infected individual are either asymptomatic or protected by a vaccine.

Our model (2.1) include many previously studied compartmental models that have infectious, symptomatically infectious, asymptomatically infected, latent, vaccinated, quarantined, and isolated compartments. When $\alpha_1 = 1$ and $\alpha_i = 0$ for $i = 2, \ldots, n$, our model can be interpreted as a multi-staged model studied in [9], in which all new infections enter the first stage. In staged progression models, the stages are understood to have a linear sequential structure. The transfer terms ϕ_{ij}, when $i > j$, denote the rate of disease progression (forward); and when $i < j$, ϕ_{ij} denote the rate of amelioration (backward). For state-structured models, a sequential order among states is no longer essential, and different states can be regarded as parallel structures. A key difference between state-structured models and staged-progression models is that a newly infected individual can manifest in any disease state while often enters into the first disease stage.

3. Graph theory preliminaries

Graph theory provides the mathematical language and tools for describing the complex structures of state transfers and transmission.

A directed graph $(\mathcal{G}) = (V, E)$ consists of a set V of vertices and a set E of directed edges that connect ordered pairs of vertices. A nonnegative weight m_{ij} can be assigned to the directed edge (i, j) from vertex j to i, then we obtain a weighted directed graph associated with weight matrix $M = (m_{ij})$, $\mathcal{G}(M) = (V, E, M)$. A directed edge (i, j) exists if and only if $m_{ij} > 0$. On the other hand, given a $n \times n$ nonnegative matrix $M = (m_{ij})$, we obtain a weighted directed graph $\mathcal{G}(M) = (V, E, M)$ with n vertices. For simplicity of notation, we will suppress the vertex and edge sets from the notation $\mathcal{G}(M)$ of a directed graph, only focus on its weight matrix M. Directed graph $\mathcal{G}(M)$ is said to be *strongly connected* if each pair of vertices are joint by a directed path.

A nonnegative matrix $M = (m_{ij})$ is *reducible* if there exists permutation matrix P such that

$$P^{-1}MP = \begin{pmatrix} M_{11} & 0 \\ M_{21} & M_{22} \end{pmatrix},$$

where M_{11} and M_{22} are square matrices. Matrix M is irreducible if and only if directed graph $\mathcal{G}(M)$ is strongly connected [50].

The algebraic Laplacian matrix $L(M)$ of M is defined as:

$$L(M) = \begin{pmatrix} \sum_{k\neq 1} m_{1k} & -m_{12} & \cdots & -m_{1n} \\ -m_{21} & \sum_{k\neq 2} m_{2k} & \cdots & -m_{2n} \\ \vdots & \vdots & \ddots & \vdots \\ -m_{n1} & -m_{n2} & \cdots & \sum_{k\neq n} m_{nk} \end{pmatrix}.$$

For each $1 \le i \le n$, let τ_i denote the co-factor of the ith diagonal entry of $L(M)$. Kirchhoff's Matrix Tree Theorem gives a graph-theoretic description of co-factor τ_i [51]. Let $\mathbb{T}_i$ be the set of all spanning sub-trees $\mathcal{T}$ of $\mathcal{G}(M)$ that are rooted at vertex i, and $w(\mathcal{T})$ be the weight of $\mathcal{T}$, the product of weights on all edges of $\mathcal{T}$.

Proposition 3.1 (*Matrix Tree Theorem [52]*). *Assume that $n \ge 2$. Then*

$$\tau_i = \sum_{\mathcal{T}\in\mathbb{T}_i} w(\mathcal{T}), \qquad i = 1, 2, \ldots, n. \tag{3.1}$$

Furthermore, if $\mathcal{G}(M)$ is strongly connected, then $\tau_i > 0$, for $i = 1, 2, \ldots, n$.

Let $F_{ij}(x)$, $1 \le i, j \le n$, $x \in \mathbb{R}^n$ be a set of functions, and $\mathbb{Q}$ the set of all spanning unicyclic subgraphs of $\mathcal{G}(M)$, with a unique directed cycle $\mathcal{C}_{\mathcal{Q}}$. Let $w(\mathcal{Q})$ be the weight of $\mathcal{Q}$ and $E(\mathcal{C}_{\mathcal{Q}})$ the set of arcs in $\mathcal{C}_{\mathcal{Q}}$. The following tree cycle identity was first derived and proved in [44,53].

Proposition 3.2 (*Tree Cycle Identity [44,53]*). *Assume that $n \ge 2$ and τ_i is given in Proposition 3.1. Then the following identity holds:*

$$\sum_{i,j=1}^{n} \tau_i m_{ij} F_{ij}(x) = \sum_{\mathcal{Q}\in\mathbb{Q}} w(\mathcal{Q}) \sum_{(s,r)\in E(\mathcal{C}_{\mathcal{Q}})} F_{rs}(x). \tag{3.2}$$

The identity in the next corollary was first given in [44] and follows from the tree cycle identity.

Proposition 3.3. *Let $\{G_i(x_i)\}_{i=1}^n$ be any family of functions, and m_{ij}, τ_i are given in Proposition 3.1. Then the following identity holds:*

$$\sum_{i,j=1}^{n} \tau_i m_{ij} G_i(x_i) = \sum_{i,j=1}^{n} \tau_i m_{ij} G_j(x_j). \tag{3.3}$$

4. Equilibria and the basic reproduction number

4.1. Equilibria

Set

$$\psi_i(I_i) = \sum_{j=1}^{n} \phi_{ji}(I_i) + \gamma_i(I_i) + \zeta_i(I_i), \quad 1 \le i \le n. \tag{4.1}$$

By assumptions (H_4)-(H_6), $\psi_i(I_i) = 0$ if and only if $I_i = 0$, for $1 \le i \le n$. System (2.1) can be rewritten as the following:

$$\begin{aligned} S' &= \theta(S) - f(N)\sum_{j=1}^{n} g_j(S, I_j), \\ I_i' &= \alpha_i f(N)\sum_{j=1}^{n} g_j(S, I_j) + \sum_{j=1}^{n} \phi_{ij}(I_j) - \psi_i(I_i), \quad i = 1, \ldots, n. \end{aligned} \tag{4.2}$$

It follows from assumptions (H_1)-(H_6) that the disease-free equilibrium $P_0 = (\bar{S}, 0, \ldots, 0)$ always exists. Let $P^* = (S^*, I_1^*, \ldots, I_n^*)$ denote a possible endemic equilibrium of (4.2). Then, the coordinates $S^*, I_1^*, \ldots, I_n^*$ are positive solutions to the following system of equilibrium equations:

$$\begin{aligned} \theta(S^*) &= f(N^*)\sum_{j=1}^{n} g_j(S^*, I_j^*), \\ \psi_i(I_i^*) &= \alpha_i f(N^*)\sum_{j=1}^{n} g_j(S^*, I_j^*) + \sum_{j=1}^{n} \phi_{ij}(I_j^*), \quad i = 1, \ldots, n, \\ N^* &= S^* + I_1^* + \cdots + I_n^*. \end{aligned} \tag{4.3}$$

We note that endemic equilibria of model (4.2) can be of two different forms: either a positive endemic equilibrium for which $I_j^* > 0$ for all $1 \le j \le n$, or a mixed endemic equilibrium for which $I_j^* > 0$ for some j and $I_j^* = 0$ for the remaining j. A positive endemic equilibrium belongs to the interior of Γ and a mixed endemic equilibrium belongs to the boundary of Γ. In the case of a positive equilibrium, the disease is endemic among all states, while in the case of a mixed endemic equilibrium, the disease is only endemic among a subset of states, and the remaining states are disease free. It was known in the literature that complex disease models can have mixed endemic equilibria (see e.g. [54,55]). It was pointed out in [55] that mixed endemic equilibria exist when the transmission network of the disease is not strongly connected. Let

$$w_{ij}(S, I_1, \ldots, I_n) = \alpha_i f(N) g_j(S, I_j) + \phi_{ij}(I_j). \tag{4.4}$$

Using assumptions (H_7) and (H_8), we define

$$m_{ij} = \lim_{S\to\bar{S}, I_j\to 0^+} \frac{w_{ij}(S, I_1, \ldots, I_n)}{I_j} = \alpha_i f(\bar{S}) c_j + b_{ij}, \tag{4.5}$$

where

$$\alpha_i f(\bar{S}) c_j = \lim_{S\to\bar{S}, I_j\to 0^+} \frac{\alpha_i f(N) g_j(S, I_j)}{I_j},$$

$$b_{ij} = \lim_{S\to\bar{S}, I_j\to 0^+} \frac{\phi_{ij}(I_j)}{I_j},$$

and let $M = (m_{ij})$ and $B = (b_{ij})$.

In weights m_{ij} defined in (4.5), the term $\alpha_i f(\bar{S}) c_j$ comes from the transmission, and the term b_{ij} defines the state-transfer matrix B. The directed graph $\mathcal{G}(M)$ is called the *transmission–transfer network* of our model (4.2), and the directed graph $\mathcal{G}(B)$ is the *state-transfer network*. From (4.5) we see that $\mathcal{G}(M)$ and $\mathcal{G}(B)$ have the same vertex set, but not necessarily the same edge set. Furthermore, if $\mathcal{G}(B)$ is strongly connected, so is $\mathcal{G}(M)$, but the inverse may not be true.

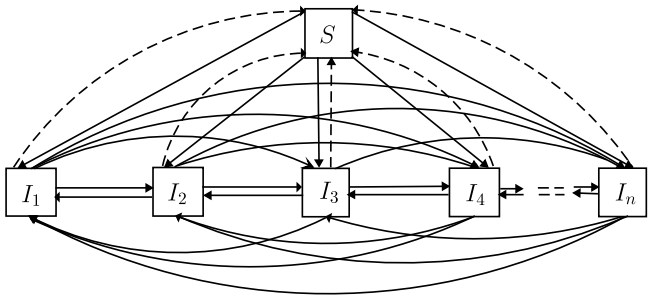

Fig. 2. The augmented directed graph with a vertex S added as a realization of the transmission–transfer network for model (4.2). The vertex S is added to demonstrate that the additional weight $\alpha_i f(\bar{S})c_j$ on the edge from I_j to I_i is created indirectly through infection of S by I_j indicated by a dashed edge from I_j to S, and the corresponding incidence in I_i indicated by a solid edge from S to I_i.

We note that the weight matrix M of the transmission–transfer network $\mathcal{G}(M)$ is obtained using the limiting values of weight functions $w_{ij}(S, I_1, \ldots, I_n)/I_j$ in (4.4) when point $(S, I_1, \ldots, I_n)$ approaches P_0. In later sections, we will also consider weight matrices $\bar{M} = (w_{ij}(S^*, I_1^*, \ldots, I_n^*))_{n\times n}$ with w_{ij} measured at endemic equilibrium $(S^*, I_1^*, \ldots, I_n^*)$ in Γ. By assumptions (H_3)-(H_8), it can be verified that directed graph $\mathcal{G}(\bar{M})$ is strongly connected if and only if the transmission–transfer network $\mathcal{G}(M)$ is strongly connected.

In Fig. 2, we show a more intuitive visualization of the transmission–transfer network: the vertex i is labelled as I_i and an additional vertex S is added so that the resulting directed graph with $(n + 1)$ vertices can be easily identified from the transfer diagram of model (2.1) in Fig. 1. We call this new directed graph by adding vertex S an *augmented directed graph* of $\mathcal{G}(M)$. In the weight m_{ij} from I_j to I_i in (4.5), b_{ij} represents the populations transfer from state j to state i. The $\alpha_i f(\bar{S})c_j$ term is less intuitive as weight from state j to i. In the augmented directed graph with $(n + 1)$ vertices in Fig. 2, we can see that this term is created indirectly through infection of S by I_j as indicated by a dashed edge from I_j to S, together with the corresponding incidence in I_i as indicated by a solid edge from S to I_i. This is also explained in Fig. 3-(b) and Fig. 3-(d). It can be verified that the weighted directed graph $\mathcal{G}(M)$ is strongly connected if and only if its augmented directed graph in Fig. 2 is strongly connected.

In Fig. 3, using a simple SEIR model, we illustrate the relations between the model transfer diagram, the augmented directed graph, the state-transfer diagram and transmission–transfer network. We note that the transmission–transfer network in Fig. 3-(d) is strongly connected, while the state-transfer network between the latent state E and infectious state I in Fig. 3-(c) only contains a single arrow from E to I, and is not strongly connected.

Proposition 4.1. *Assume that the transmission–transfer network $\mathcal{G}(M)$ of (4.2) is strongly connected. Then the disease-free equilibrium $P_0 = (\bar{S}, 0, \ldots, 0)$ is the only equilibrium of (4.2) on the boundary of $\mathbb{R}^{n+1}$.*

Proof. The proof is similar to that of Theorem 2.3 in [55], in which only a transmission network is considered. It suffices to exclude the existence of mixed endemic equilibria on the boundary of Γ.

Let $P^* = (S^*, I_1^*, \ldots, I_n^*)$ denote a nonnegative equilibrium of (4.2), where $S^* \geq 0, I_j^* \geq 0, 1 \leq j \leq n$. Using assumption (H_1) and the first equilibrium equation of (4.3), we have $S^* > 0$.

If an arc from j to i exists and $I_j^* > 0$, we show that $I_i^* > 0$. Assume otherwise that $I_i^* = 0$, then assumptions (H_4)-(H_6) imply that $\psi_i(I_i^*) = 0$, and assumption (H_3) and $I_j^* > 0$ imply that $g_j(S^*, I_j^*) > 0$. Using the equation for I_i we obtain

$$I_i'|_{P^*} = \alpha_i f(N^*) \sum_{k=1}^{n} g_k(S^*, I_k^*) + \sum_{k=1}^{n} \phi_{ik}(I_k^*) \geq \alpha_i f(N^*) g_j(S^*, I_j^*) > 0.$$

This contradicts the fact that P^* is an equilibrium, and shows $I_i^* > 0$.

If an oriented path $(j, j_1, \ldots, j_k, i)$ from j to i exists and $I_j^* > 0$, using statement above repeatedly, we can show that $I_i^* > 0$.

Since the transmission–transfer network $\mathcal{G}(M)$ is strongly connected, for given two states i, j, there exists and oriented path from j to i and from i to j. From the preceding arguments, we know that $I_j^* > 0$ implies $I_i^* > 0$. Therefore, $I_j^* > 0$ for some j implies $I_i^* > 0$ for all i, namely, for all $1 \leq j \leq n$, I_j^* are either all zero or all positive, and thus the only equilibrium on the boundary is the disease-free equilibrium P_0. □

If $\mathcal{G}(M)$ is not strongly connected, then there may exist a state i that can reach other states but is not reachable from any other state. Then, when $I_i^* = 0$, there exist state j for which $I_j^* > 0$, and mixed endemic equilibria exist on the boundary. We give the following example to demonstrate this.

Example 4.1. Consider the epidemic model (4.6) illustrated by the transfer diagram in Fig. 4(a). Its transmission–transfer network is not strongly connected, and it has two boundary equilibria.

To see the claims in Example 4.1, we note that the state I_2 is not reachable from any other states either by state transfer or transmission, and the transmission–transfer network is not strongly connected (Fig. 4). The node I_2 in the transfer diagram (Fig. 4(a)) can be thought of as an external source of infections that feeds into the system $S - I_1 - R$, and the external infection source is not sustainable due to effective control measures. This can be the case when other regions have the epidemics under control and the importations into the region from outside will dwindle to zero. From the model equation (4.6) we can see that two boundary equilibria can exist: the disease-free equilibrium $P_0 = (\bar{S}, 0, 0, 0)$, a mixed endemic equilibrium $(S^*, I_1^*, 0, R^*)$, $S^*, I_1^*, R^* > 0$.

$$\begin{aligned} S' &= \Lambda - \beta I_1 S - dS \\ I_1' &= \beta I_1 S - (d_1 + \gamma_1) I_1 + \alpha I_2 \\ I_2' &= -(d_2 + \alpha) I_2 \\ R' &= \gamma_1 I_1 - dR. \end{aligned} \tag{4.6}$$

In this paper, we only consider the case when the transmission-transfer network $\mathcal{G}(M)$ is strongly connected. In the case when $\mathcal{G}(M)$ is not strongly connected, the dynamics of model (4.2) can be analysed following the approach in [55] using the condensed graph.

4.2. The basic reproduction number $\mathcal{R}_0$

The basic reproduction number $\mathcal{R}_0$ is the expected number of secondary infections produced by a typical infectious individual during its entire infectious period in an entirely susceptible population. The mathematical definition of the basic reproduction number is by the spectral radius of the next generation matrix, see [56,57].

Let $\psi_i(I_i)$ be defined at the beginning of Section 4.1 and

$$b_{ii} := \lim_{I_i \to 0^+} \frac{\psi_i(I_i)}{I_i} = \sum_{j=1, j\neq i}^{n} b_{ji} + a_i > 0, \quad 1 \leq i \leq n. \tag{4.7}$$

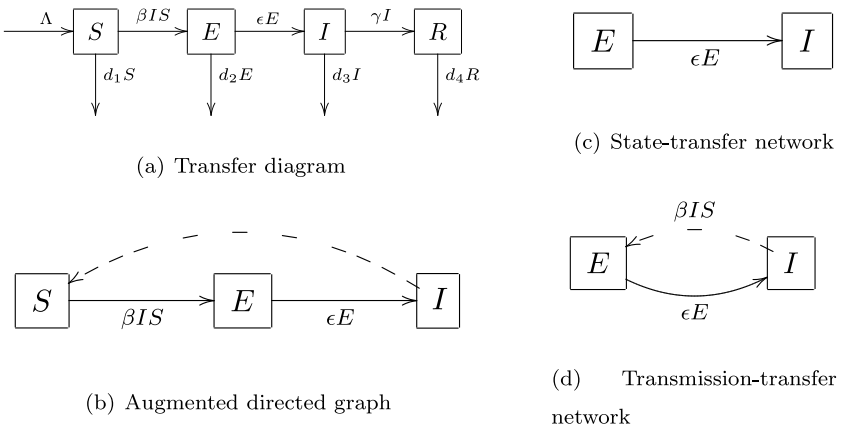

(a) Transfer diagram (c) State-transfer network

(b) Augmented directed graph (d) Transmission-transfer network

Fig. 3. The transfer diagram (a) of an SEIR model, its augmented directed graph (b), state-transfer network (c) and transmission–transfer network (d).

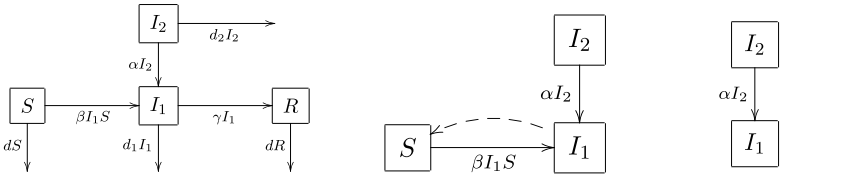

(a) Transfer diagram (b) Augmented direct graph (c) Transmission-transfer network

Fig. 4. The transfer diagram (a), augmented direct graph (b), and transmission–transfer network (c) of model (4.6) are shown. The node I_2 is an unsustainable external source of infection that feeds into the SI_1R system but does not receive feedback. The term αI_2 can be interpreted as importations of infections from other regions that have implemented effective control measures. The augmented direct graph in (b) is not strongly connected because other nodes cannot reach I_2, and correspondingly, the transmission–transfer network in (c) is not strongly connected. The model (4.6) has two boundary equilibria.

Following [57], the basic reproduction number for model (4.2) is the spectral radius (dominant eigenvalue) of next generation matrix FV^{-1},

$$\mathcal{R}_0 = \rho(FV^{-1}), \tag{4.8}$$

where $\rho(A)$ denotes the spectral radius of a matrix A, and

$$\begin{aligned} F &= f(\bar{S}) \begin{pmatrix} \alpha_1 c_1 & \alpha_1 c_2 & \cdots & \alpha_1 c_n \\ \alpha_2 c_1 & \alpha_2 c_2 & \cdots & \alpha_2 c_n \\ \vdots & \vdots & \ddots & \vdots \\ \alpha_n c_1 & \alpha_n c_2 & \cdots & \alpha_n c_n \end{pmatrix}, \\ V &= \begin{pmatrix} b_{11} & -b_{12} & \cdots & -b_{1n} \\ -b_{21} & b_{22} & \cdots & -b_{2n} \\ \vdots & \vdots & \ddots & \vdots \\ -b_{n1} & -b_{n2} & \cdots & b_{nn} \end{pmatrix}. \end{aligned} \tag{4.9}$$

Using (4.7), (H_8) and (H_9), it can be verified that F is a nonnegative matrix, and V is a nonsingular M-matrix with a nonnegative inverse V^{-1}.

Assumptions (H_7)-(H_9) are sufficiently weak to allow the nonlinear incidence function $g(S, I_i)$ and transfer functions ϕ_{ij}, γ_i, and ζ_i to be not differentiable at the disease-free equilibrium. For instance, a common incidence function $g_i(S, I_i) = \sum_{j=1}^{n} \lambda_i S I_j^p$ satisfies these assumptions with $0 < p < 1$, but it is not differentiable at $I_i = 0$. When these functions are differentiable at $I_i = 0$, constants c_i, b_{ij} are given by the corresponding derivatives at $I_i = 0$.

In the most common case when $f(N) \equiv 1$, $g_j(S, I_j) = \beta_j S I_j$, $\phi_{ij}(I_j) = \delta_{ij} I_j$, $\gamma_i(I_i) = \gamma_i I_i$ and $\zeta_i(I_i) = d_i I_i$, assumptions (H_7)-(H_9) are automatically satisfied with

$$c_i = \beta_i \bar{S}, \quad b_{ij} = \delta_{ij}, \quad a_i = \gamma_i + d_i > 0, \quad b_{ii} = \sum_{j=1, j\neq i}^{n} \delta_{ji} + \gamma_i + d_i > 0. \tag{4.10}$$

It can be verified that the definition of basic reproduction number $\mathcal{R}_0$ in (4.8) includes as special cases the corresponding definitions for simpler models in the literature (see e.g. [5–9,46,47,58,59]).

4.3. Biological interpretations of $\mathcal{R}_0$

The basic reproduction number in (4.12) can be interpreted as the sum of the expected number of secondary infections contributed by an infected individual at each infection state.

Proposition 4.2. *Suppose that assumptions* (H_1)-(H_9) *hold. Let*

$$(w_1, w_2, \ldots, w_n) = \big(f(\bar{S})c_1, f(\bar{S})c_2, \ldots, f(\bar{S})c_n\big)V^{-1}. \tag{4.11}$$

Then $w_i \geq 0$, $1 \leq i \leq n$, *and* $\max_{1\leq i\leq n}\{w_i\} > 0$. *Furthermore, the following results hold:*

(i) Nonnegative matrix FV^{-1} has a unique positive eigenvalue $\rho(FV^{-1})$.
(ii) The basic reproduction number satisfies

$$\mathcal{R}_0 = \rho(FV^{-1}) = \alpha_1 w_1 + \alpha_2 w_2 + \cdots + \alpha_n w_n. \tag{4.12}$$

Proof. The matrix F can be written as

$$F = (\alpha_1, \alpha_2, \ldots, \alpha_n)^T \big(f(\bar{S})c_1, f(\bar{S})c_2, \ldots, f(\bar{S})c_n\big). \tag{4.13}$$

By (4.11) and (4.13), we have $FV^{-1} = (\alpha_1, \alpha_2, \ldots, \alpha_n)^T (w_1, w_2, \ldots, w_n)$. Then matrix FV^{-1} has rank 1, and thus its spectral

radius is the only positive eigenvalue and is equal to its trace $\alpha_1\omega_1 + \alpha_2\omega_2 + \cdots + \alpha_n\omega_n$, leading to (4.12). □

As pointed out in [57], the (k, j) entry of matrix V^{-1} represents the average time of an infected individual originally at the jth state spends in the kth state, the (i, k) entry of matrix F is the incidence rate at which an infected individual in the kth state cross infect in the ith state. Overall, the (i, j) entry of matrix FV^{-1} is the expected number of new infections into the ith state made by an infected individual of the jth state during its infectious period, accounting for the time this individual stays in all states.

As defined in (4.11), w_j is the sum of the jth column of matrix FV^{-1}, and represents the expected number of new infections produced by a newly infected individual at the jth state during its entire infectious period.

To interpret $\mathcal{R}_0$ in (4.12) biologically, consider a newly infected individual, with probability α_i the individual is at the state i, $1 \le i \le n$, and will produce expected w_i secondary infections during its infectious period. Therefore, the total expected number of secondary infections during its infectious period is

$$\mathcal{R}_0 = \alpha_1 w_1 + \cdots \alpha_n w_n.$$

Consider the special case when the proportions of incidence among states is such that $\alpha_1 = 1$, $\alpha_i = 0$ for $i = 2, \ldots, n$, namely, all new infections enter the first state. In such a case, disease states can simply represent stages of disease progression. The resulting model agrees with the staged progression model considered in [9]. By (4.12), $\mathcal{R}_0 = w_1$, which agrees with the basic reproduction number given in [9]. Similarly, if $\alpha_1 = \cdots = \alpha_n = 1/n$, then

$$\mathcal{R}_0 = \frac{w_1 + \cdots + w_n}{n}.$$

In the next result, we show that the basic reproduction number can also be interpreted using the average time spent by an infected individual at each disease state.

Proposition 4.3. *Assume that assumptions* (H_1)-(H_9) *hold. Let*

$$(T_1, T_2, \ldots, T_n)^T = V^{-1}(\alpha_1, \alpha_2, \ldots, \alpha_n)^T. \tag{4.14}$$

Then the following results hold:

(i) $T_i \ge 0$ *and* $\max_{1\le i\le n}\{T_i\} > 0$.
(ii) $T = \sum_{i=1}^n T_i$ *is the average infectious period of an infected individual.*
(iii) *The basic reproduction number* $\mathcal{R}_0$ *satisfies*

$$\mathcal{R}_0 = f(\bar{S})c_1T_1 + \cdots + f(\bar{S})c_nT_n. \tag{4.15}$$

Proof. By (4.11) and (4.12),

$$\begin{aligned}\mathcal{R}_0 &= (w_1, \ldots, w_n)(\alpha_1, \ldots, \alpha_n)^T \\ &= \big(f(\bar{S})c_1, \ldots, f(\bar{S})c_n\big)V^{-1}(\alpha_1, \ldots, \alpha_n)^T.\end{aligned}$$

Then, (4.15) follows from (4.14).

Since the (i, j) entry of matrix V^{-1} represents the average time of an infected individual originally at the jth state spends in the ith state, we know that T_i in (4.14) is the average time an infected individual spends in the ith state. For each $1 \le i \le n$, $f(\bar{S})c_i$ denotes the force of infection at the beginning of an epidemic with respect to an infected individual at the ith state, and $f(\bar{S})c_iT_i$ represents the expected number of secondary infections produced by an infectious individual who is at state i, and the basic reproduction number is given by (4.15). Moreover, $T = \sum_{i=1}^n T_i$ is the average infectious period of an infected individual. □

4.4. Upper and lower bounds on $\mathcal{R}_0$

Let c_i be defined in (4.10). Define

$$R_{0i} = \frac{f(\bar{S})c_i}{a_i} \ge 0, \quad 1 \le i \le n. \tag{4.16}$$

Biologically, R_{0i} represents the basic reproduction number of ith state when the other states are absent. For instance, when $f(N) \equiv 1$, $g_j(S, I_j) = \beta_j SI_j$, $\phi_{ij}(I_j) = \delta_{ij}I_j$, $\gamma_i(I_i) = \gamma_i I_i$ and $\zeta_i(I_i) = d_i I_i$, then we arrive at the standard expression for the basic reproduction number of a single group SIR model:

$$R_{0i} = \frac{\beta_i \bar{S}}{\gamma_i + d_i}, \quad 1 \le i \le n. \tag{4.17}$$

The following proposition gives a lower and upper bound on the basic reproduction number R_0.

Proposition 4.4. *Suppose that assumptions* (H_1)-(H_9) *hold. Then the basic reproduction number defined by* (4.12) *satisfies the following inequality:*

$$\min_{1\le i\le n}\{R_{0i}\} \le \mathcal{R}_0 \le \max_{1\le i\le n}\{R_{0i}\}. \tag{4.18}$$

Proof. Let $R_{0j} = \min_{1\le i\le n}\{R_{0i}\}$ for some $1 \le j \le n$. By (4.7) and (4.9) we obtain that $(a_1, \ldots, a_n)V^{-1} = (1, \ldots, 1)$. Since matrix V^{-1} is nonnegative and using (4.11), we have

$$(w_1, \ldots, w_n) = f(\bar{S})\frac{c_j}{a_j}\left(\frac{c_1a_j}{c_j}, \ldots, \frac{c_na_j}{c_j}\right)V^{-1} \ge R_{0j}(1, \ldots, 1).$$

By (4.12), we have $\mathcal{R}_0 = \alpha_1w_1 + \alpha_2w_2 + \cdots + \alpha_nw_n \ge \sum_{i=1}^n \alpha_iR_{0j} = R_{0j}$. Similarly, we can show $\mathcal{R}_0 = \alpha_1w_1 + \alpha_2w_2 + \cdots + \alpha_nw_n \le \max_{1\le i\le n} R_{0i}$, completing the proof. □

5. Global dynamics and threshold results

In this section we carry out analysis of the global dynamics of system (4.2), and establish a sharp threshold result: if $\mathcal{R}_0 \le 1$, then the disease-free equilibrium P_0 is globally asymptotically stable in Γ, and the disease dies out; if $\mathcal{R}_0 > 1$, and if $f(N) \equiv 1$, then the positive endemic equilibrium P^* is unique and globally asymptotically stable in the interior of Γ. In this case, the disease persists in the population and has a positive stationary distribution among all disease states. The proof relies on construction of global Lyapunov functions. We have adapted the graph-theoretic approach developed in [43,44] to system (4.2).

5.1. Global dynamics when $\mathcal{R}_0 \le 1$

We first describe the Lyapunov function for the case $\mathcal{R}_0 \le 1$.

Proposition 5.1. *Let* w_i *is defined by* (4.11). *If*

$$(I_1', I_2', \ldots, I_n')^T \le (F - V)(I_1, I_2, \ldots, I_n)^T \tag{5.1}$$

holds in Γ, *and* $\mathcal{R}_0 \le 1$, *then*

$$L(I_1, I_2, \ldots, I_n) = (w_1, w_2, \ldots, w_n)(I_1, I_2, \ldots, I_n)^T \tag{5.2}$$

is a Lyapunov function for system (4.2) *in* Γ, *namely,*

$$\frac{d}{dt}L(I_1(t), I_2(t), \ldots, I_n(t)) \le 0, \quad \text{for all } t \ge 0,$$

along all solutions of (4.2) *in* Γ.

Proof. Differentiating function $L(t) = L(I_1(t), \ldots, I_n(t))$ with respect to t, we have

$$\begin{aligned}\dot{L} &\le (w_1, \ldots, w_n)(F - V)(I_1, \ldots, I_n)^T \\ &= (w_1, \ldots, w_n)(\alpha_1, \ldots, \alpha_n)^T \big(f(\bar{S})c_1, \ldots, f(\bar{S})c_n\big)(I_1, \ldots, I_n)^T \\ &\quad - (w_1, \ldots, w_n)V(I_1, \ldots, I_n)^T.\end{aligned}$$

Using (4.11) and (4.12) we obtain

$$\begin{aligned}\dot{L} &\le \mathcal{R}_0\big(f(\bar{S})c_1, \ldots, f(\bar{S})c_n\big)(I_1, \ldots, I_n)^T \\ &\qquad - \big(f(\bar{S})c_1, \ldots, f(\bar{S})c_n\big)V^{-1}V(I_1, \ldots, I_n)^T \\ &= (\mathcal{R}_0 - 1)\big(f(\bar{S})c_1, \ldots, f(\bar{S})c_n\big)(I_1, I_2, \ldots, I_n)^T \\ &= (\mathcal{R}_0 - 1)f(\bar{S})\sum_{i=1}^{n} c_i I_i \le 0,\end{aligned}$$

completing the proof. □

We make the following assumptions:

- (A_1) For $1 \le i \le n$, $f(S)g_i(S, I_i) \le f(\bar{S})g_i(\bar{S}, I_i)$ holds for all $0 \le S \le \bar{S}$, $I_i \ge 0$; if $f(S)g_i(S, I_i) = f(\bar{S})g_i(\bar{S}, I_i) \not\equiv 0$, then $S = \bar{S}$; for $I_i > 0$, $\frac{g_i(\bar{S}, I_i)}{I_i} \le c_i$.
- (A_2) For all $I_j > 0$, $1 \le i, j \le n$, $i \ne j$, $\sup_{I_j>0} \frac{\phi_{ij}(I_j)}{I_j} = b_{ij}$; for all $I_i > 0$, $1 \le i \le n$, $\inf_{I_i>0} \frac{\psi_i(I_i)}{I_i} = b_{ii}$.

It can be verified that these assumptions are satisfied by common incidence forms and linear transfer functions. Since biologically the incidence function $g_i(S, I_i)$ should be nondecreasing in S, assumption (A_1) is satisfied if either $f(N) \equiv 1$ or $g_i(S, I_i)$ is strictly increasing in S. Under assumptions (A_1) and (A_2), we can show that condition (5.1) is satisfied and the function L defined in (5.2) is a Lyapunov function as stated in the next result. The proof is technical and is given in the Appendix.

Corollary 5.1. *Assume that* (A_1) *and* (A_2) *hold. Then function* $L = \sum_{i=1}^{n} \omega_i I_i$ *is a Lyapunov function for system* (4.2) *in* Γ.

Theorem 5.1. *Suppose that assumptions* (H_1)-(H_9) *are satisfied. The following statements hold:*

(a) *If* $\mathcal{R}_0 \le 1$ *and* (A_1), (A_2) *hold, then the disease-free equilibrium* P_0 *is globally asymptotically stable in* Γ.
(b) *If* $\mathcal{R}_0 > 1$ *then the disease-free equilibrium* P_0 *is unstable. Furthermore, if the transmission–transfer network of model* (4.2) *is strongly connected, then system* (4.2) *is uniformly persistent with respect to the interior of* Γ.

Proof. By Corollary 5.1, function $L = \sum_{i=1}^{n} w_i I_i$ is a Lyapunov function for (4.2), and

$$\dot{L} \le (\mathcal{R}_0 - 1)f(\bar{S})\sum_{i=1}^{n} c_i I_i \le 0,$$

for all $(S, I_1, \ldots, I_n) \in \Gamma$. Let K be the largest invariant subset of $\{(S, I_1, \ldots, I_n) \in \Gamma : \dot{L} = 0\}$. Then $P_0 \in K$. Let $(S(t), I_1(t), \ldots, I_n(t))$ be a solution in K. We consider two cases. Case (1): $\mathcal{R}_0 < 1$. In this case, $\dot{L} = 0$ if and only if $f(\bar{S})\sum_{i=1}^{n} c_i I_i = 0$. By assumption ($A_1$), this means that $\sum_{i=1}^{n} g_i(S, I_i) = 0$, hence $\theta(S) = 0$, and $S = \bar{S}$. Using assumption (H_5), we have

$$\sum_{i=1}^{n} I_i' = -\sum_{i=1}^{n} \gamma_i(I_i) - \sum_{i=1}^{n} \zeta_i(I_i) \le -\sum_{i=1}^{n} \zeta_i(I_i) \le -\sum_{i=1}^{n} d_i I_i. \quad (5.3)$$

Therefore, $I_i = 0$ for all i. Case (2): $\mathcal{R}_0 = 1$. In this case, $\dot{L} = 0$ implies $f(S)g_i(S, I_i) = f(\bar{S})g_i(\bar{S}, I_i) \not\equiv 0$, and thus $S = \bar{S}$ by assumption (A_1). Moreover, along any solution in K, $\sum_{i=1}^{n} g_i(S, I_i) = 0$ holds. Using the same procedure as in Case (1), we obtain that $I_i = 0$ for all i. In both cases, we have shown that $K = \{P_0\}$. By LaSalle's Invariance Principle [60], P_0 is globally asymptotically stable in Γ when $\mathcal{R}_0 \le 1$. This establishes part (a).

If $\mathcal{R}_0 > 1$, then, by continuity, $\dot{L} > 0$ for S sufficiently close to $\bar{S}$ except when $I_1 = I_2 = \cdots = I_n = 0$. Solutions starting sufficiently close to P_0 leave a small neighbourhood of P_0, except for those on the invariant S-axis. Since the transmission–transfer network of model (4.2) is strongly connected, P_0 is the only equilibrium on the boundary of Γ by Proposition 4.1. By a uniform persistence result, Theorem 4.3 in [61], and using a similar proof of Proposition 3.3 in [62], we can show that instability of P_0 is equivalent to the uniform persistence of system (4.2) with respect to the interior of Γ. This completes the proof. □

Uniform persistence of system (4.2) in Γ and uniform ultimate boundedness of solutions in Γ imply that there exists an equilibrium in the interior of Γ, see [63] (Theorem D.3) or [64] (Theorem 2.8.6).

Corollary 5.2. *Suppose that assumptions* (H_1) - (H_9) *hold. Assume that* $\mathcal{R}_0 > 1$ *and that the transmission–transfer network of system* (4.2) *is strongly connected. Then system* (4.2) *has an endemic equilibrium in the interior of* Γ.

The assumption that the transmission–transfer network is strongly connected is necessary for ruling out boundary equilibria other than P_0, and in turn, crucial for the proof of uniform persistence and existence of positive endemic equilibrium P^* when $\mathcal{R}_0 > 1$. This condition was neglected in many earlier work on complex epidemic models.

5.2. Global dynamics when $\mathcal{R}_0 > 1$

We assume that $f(N) \equiv 1$ in this subsection and establish that, when $\mathcal{R}_0 > 1$, system (4.2) has a unique endemic equilibrium P^* and it is globally asymptotically stable in the interior of Γ.

System (4.2) is a large-scale system of nonlinear equations. Proof of global stability for systems of this type is typically done using the method of Lyapunov functions. The graph-theoretic approach for constructing global Lyapunov functions developed in [43,44] has been successfully applied to many complex systems. An application of the approach to multi-staged models was shown in [9]. Comparing to the multi-stage model in [9], system (4.2) has disease incidence terms in all I_i equations and are more interconnected. The graph-theoretic approach needs to be adapted to (4.2) to resolve its global-stability problem.

Let $P^* = (S^*, I_1^*, \ldots, I_n^*)$, $I_1^*, \ldots, I_n^* > 0$, be an endemic equilibrium. Using the weight function $w_{ij}(S, I_1, \ldots, I_n)$ in (4.5), we define a nonnegative matrix $\bar{M} = (\bar{m}_{ij})_{n\times n}$, with

$$\bar{m}_{ij} = w_{ij}(S^*, I_1^*, \ldots, I_n^*) = \alpha_i g_j(S^*, I_j^*) + \phi_{ij}(I_j^*), \quad 1 \le i, j \le n. \quad (5.4)$$

The corresponding weighted directed graph $\mathcal{G}(\bar{M})$ has the same vertex and edge sets as the transmission–transfer network $\mathcal{G}(M)$ in Section 4.1, but the weights are measured at the endemic equilibrium P^*. Using (H_3) and (H_4), we know that $\mathcal{G}(M)$ is strongly connected if and only if $\mathcal{G}(\bar{M})$ is strongly connected.

Motivated by method in [9], we construct a candidate Lyapunov function of form

$$V(S, I_1, I_2, \ldots, I_n) = \bar{\tau}\int_{S^*}^{S} \frac{\Phi(\xi) - \Phi(S^*)}{\Phi(\xi)} d\xi + \sum_{i=1}^{n} \tau_i \int_{I_i^*}^{I_i} \frac{\psi_i(\xi) - \psi_i(I_i^*)}{\psi_i(\xi)} d\xi, \quad (5.5)$$

where τ_i is given in Proposition 3.1 and $\bar{\tau} = \sum_{i=1}^{n} \tau_i \alpha_i$. In the special case when $\alpha_1 = 1$, and $\alpha_i = 0$ for $i = 2, \ldots, n$, the

Lyapunov function in (5.5) reduces to the Lyapunov function for the staged progression model in [9]. The proof of our next result is technical and provided in the Appendix.

Proposition 5.2. *Assume that $f(N) \equiv 1$. Suppose that there exists Lipschitz continuous function $\Phi : \mathbb{R}_+ \to \mathbb{R}_+$ such that the following assumptions hold:*

(B_1) *For $S \neq S^*$, $S > 0$,*

$$\big(\theta(S) - \theta(S^*)\big)\big(\Phi(S) - \Phi(S^*)\big) < 0;$$

(B_2) *For $0 \le S \le \bar{S}$, $I_j > 0$, $1 \le j \le n$,*

$$\left(\frac{g_j(S,I_j)}{\Phi(S)} - \frac{g_j(S^*,I_j^*)}{\Phi(S^*)}\right)\left(\frac{g_j(S,I_j)}{\Phi(S)\psi_j(I_j)} - \frac{g_j(S^*,I_j^*)}{\Phi(S^*)\psi_j(I_j^*)}\right) \le 0;$$

(B_3) *For $I_j > 0$, $1 \le i, j \le n$,*

$$\big(\phi_{ij}(I_j) - \phi_{ij}(I_j^*)\big)\left(\frac{\phi_{ij}(I_j)}{\psi_j(I_j)} - \frac{\phi_{ij}(I_j^*)}{\psi_j(I_j^*)}\right) \le 0.$$

Then the function V defined in (5.5) is a Lyapunov function for system (4.2) with respect to the interior of Γ.

We remark that assumption (B_3) is automatically satisfied if transfer functions ϕ_{ij} and ψ_j are linear. If the incidence function is of separable form $g_j(S, I_j) = p(S)q_j(I_j)$, we can choose $\Phi(S) = p(S)$. Then assumption (B_2) is satisfied if $q_i(I_j)$ is strictly increasing in I_j, as in the case for $q_j(I_j) = I_j^p$ or $q_j(I_j) = \frac{I_j^p}{1+aI_j^p}$, $p \ge 0$, $a \ge 0$. If the growth function takes the form $\theta(S) = \Lambda - dS$, then assumption (B_1) is satisfied if Φ is strictly increasing in S.

For our next result, we make the following assumption, which is satisfied by common incidence functions and linear transfer functions.

(B_4) For each $1 \le i \le n$, one of the functions $g_i(S^*, I_i)$, $\sum_{j=1}^n \phi_{ij}(I_j)$, $\psi_i(I_i)$ is strictly monotone in $I_i > 0$.

Theorem 5.2. *Suppose that assumptions (H_1)-(H_9), (B_1)-(B_4) hold, $f(N) \equiv 1$, and the transmission–transfer network of model (4.2) is strongly connected. If $\mathcal{R}_0 > 1$, then the positive endemic equilibrium P^* is unique and globally asymptotically stable in the interior of Γ.*

Proof. Choose the Lyapunov function defined by (5.5). Then $\dot{V} \le 0$ in the interior of Γ by Proposition 5.2. Moreover, $\dot{V} = 0$ implies that

$$\left(1 - \frac{\Phi(S^*)}{\Phi(S)}\right)\Big(\theta(S) - \theta(S^*)\Big) = 0,$$

and thus $S = S^*$ by assumption (B_1). Since $s(x) = 1 - x + \ln x$ has a global maximum 0 at $x = 1$, we obtain that, for some constant $\lambda > 0$,

$$\frac{g_j(S^*,I_j)}{g_j(S^*,I_j^*)} = \frac{\psi_j(I_j)}{\psi_j(I_j^*)} = \frac{\phi_{ij}(I_j)}{\phi_{ij}(I_j^*)} = \lambda, \tag{5.6}$$

hold for all $I_j > 0$, $1 \le j \le n$. Therefore, along solutions that stay in the largest invariant subset of $\{(S, I_1, \ldots, I_n) \in \Gamma \ : \ \dot{V} = 0\}$, the following relation holds

$$S = S^*, \quad g_j(S^*, I_j) = \lambda g_j(S^*, I_j^*).$$

Using the S-equation in system (4.2), we have

$$0 = \theta(S^*) - \lambda \sum_{j=1}^n g_j(S^*, I_j^*).$$

This equation holds only at $\lambda = 1$. Substituting $\lambda = 1$ into (5.6), we obtain

$$g_j(S^*, I_j) = g_j(S^*, I_j^*), \ \ \psi_j(I_j) = \psi_j(I_j^*), \ \ \phi_{ij}(I_j) = \phi_{ij}(I_j^*).$$

The monotonicity assumption (B_4) implies that $I_i = I_i^*$ for all i. Thus, the largest invariant set in the set $\{\dot{V} = 0\}$ is the singleton $\{P^*\}$. By LaSalle's Invariance Principle [60], P^* is globally asymptotically stable in the interior of Γ. The global stability also implies that the endemic equilibrium is unique. □

We note that in the case when all newly infected individuals go into the first state, namely, $\alpha_1 = 1$, $\alpha_i = 0$, $2 \le i \le n$, Theorems 5.1 and 5.2 give the global-stability results in [9].

We also note that, if $f(N)$ is a nonconstant function, the global stability of P^* when $\mathcal{R}_0 > 1$ remains largely open, even for the case when $f(N)$ is monotone. For certain non-monotone functions $f(N)$, it was shown in [49] that multiple endemic equilibria can exist and periodic oscillations can occur, and the global stability results are not expected to be valid.

6. Numerical investigations and discussions

Results from numerical simulations are provided in this section to demonstrate our theoretical results. Several observations are made regarding the impacts of state structures on the dynamics. As we will show, some of the observations shed interesting lights on the impacts of state structure and raise interesting questions for further theoretical studies.

To focus our study on the state structure, we choose a simple form for functions f, g, ϕ and ψ in model (4.2). We let $n = 5$ and consider a special star-shaped directed graph for cross-transmissions among the 5 states, as shown in Fig. 6-(a). The corresponding weight matrix $\bar{M} = (\bar{m}_{ij})_{5\times 5}$ is given by

$$\bar{m}_{ij} = \alpha_i\beta_j S^* I_j^* + \delta_{ij} I_j^*, \ \ 1 \le i, j \le 5$$

is irreducible. The simplified model is described by the following systems of differential equations:

$$\begin{aligned}
S' &= \Lambda - dS - \sum_{j=1}^5 \beta_j S I_j,\\
I_1' &= \alpha_1 \sum_{j=1}^5 \beta_j S I_j + \delta_{12} I_2 + \delta_{13} I_3 + \delta_{14} I_4 + \delta_{15} I_5\\
&\qquad - (\delta_{21} + \delta_{31} + \delta_{41} + \delta_{51} + \gamma_1 + d) I_1,\\
I_2' &= \alpha_2 \sum_{j=1}^5 \beta_j S I_j + \delta_{21} I_1 - (\delta_{12} + \gamma_2 + d) I_2,\\
I_3' &= \alpha_3 \sum_{j=1}^5 \beta_j S I_j + \delta_{31} I_1 - (\delta_{13} + \gamma_3 + d) I_3,\\
I_4' &= \alpha_4 \sum_{j=1}^5 \beta_j S I_j + \delta_{41} I_1 - (\delta_{14} + \gamma_4 + d) I_4,\\
I_5' &= \alpha_5 \sum_{j=1}^5 \beta_j S I_j + \delta_{51} I_1 - (\delta_{15} + \gamma_5 + d) I_5.
\end{aligned} \tag{6.1}$$

It can be verified that all assumptions (H_1)-(H_9) in Section 2, (A_1)-(A_2) and (B_1)-(B_4) in the previous sections are automatically satisfied by model (6.1). From the results in Section 5 we know that the disease-free equilibrium P_0 is globally asymptotically stable if $\mathcal{R}_0 \le 1$, and that, when $\mathcal{R}_0 > 1$, there exists a unique positive endemic equilibrium $P^* = (S^*, I_1^*, \ldots, I_5^*)$ and it is globally asymptotically stable.

Model (6.1) can be regarded as an approximation for the transmission dynamics of HIV infection with treatment among an

adult population. We have chosen the following parameter values based on those in [4,65]:

$$\begin{aligned}&\Lambda = 800,\ d = 0.02,\ (\alpha_1, \alpha_2, \alpha_3, \alpha_4, \alpha_5)\\&\quad = (0.3, 0.4, 0.2, 0.08, 0.02),\\&(\delta_{21}, \delta_{31}, \delta_{41}, \delta_{51}, \delta_{12}, \delta_{13}, \delta_{14}, \delta_{15})\\&\quad = (0.2, 0.2, 0.2, 0.2, 0.3, 0.3, 0.3, 0.3),\\&(\gamma_1, \gamma_2, \gamma_3, \gamma_4, \gamma_5) = (0.03, 0.042, 0.198, 0.32, 0.45).\end{aligned} \tag{6.2}$$

The initial populations are chosen as $(14500, 300, 200, 0, 0, 0)$. We have also selected two sets of transmission coefficients:

$$(\beta_1, \ldots, \beta_5) = (0.1070, 0.0535, 0.1605, 0.2140, 0.1338) \times 10^{-5}, \tag{6.3}$$

for which the basic reproduction number $\mathcal{R}_0 = 0.3004 < 1$; and

$$(\beta_1, \ldots, \beta_5) = (0.2140, 0.1070, 0.3210, 0.4280, 0.2675) \times 10^{-4}, \tag{6.4}$$

for which the basic reproduction number is $\mathcal{R}_0 = 6.0074 > 1$. Results in Theorems 5.1 and 5.2 are illustrated in Fig. 5.

While the parameter values in (6.2)–(6.4) were not fitted from clinical data, they are chosen in comparable scale or order of magnitude to those parameter values in two previous HIV studies [4] and [65]. In [4], detailed discussions were given on the selection of parameter values from the HIV literature for a 4-stage progression model of HIV, which helped us to choose values for state-transfer parameters that are biologically plausible for HIV progression. In [65], parameter values were fitted for a simple transmission model for the HIV for a population in a remote Chinese village, which helped us to choose values for demographic parameters and transmission coefficients. Results in the discussion are not only of general theoretical interest, but also relevant to HIV progression and control.

6.1. The impact of parameters on the distribution of disease prevalence among states

In this section, we discuss the distribution of number of infected individuals among different disease states when the dynamics have stabilized at the endemic equilibrium, as well as important factors that impact this distribution. This is a complicated problem on its own. Using numerical simulations, we provide some interesting observations. Let $P^* = (S^*, I_1^*, \ldots, I_5^*)$ be the endemic equilibrium, we are interested in factors that influence the distribution of disease prevalence I_i^* at state i given by $(I_1^*, \ldots, I_5^*)$. A specific question of interest is the following: what factor (or factors) determines that a particular I_k^* is the highest among all I_i^*? or determines the order among I_i^*? Important factors we have investigated include transmission coefficients β_i, fraction α_i of disease incidences in state i, and transfer rates ϕ_{ij} among disease states.

Observation I: Varying transmission coefficients β_i do not alter the order among the disease prevalences I_i^*, $i = 1, \ldots, 5$.

This is intuitively clear since β_i directly influence the disease incidences, which is given in the following form, for the state i:

$$\alpha_i S^* \Big(\sum_{k=1}^{5} \beta_k I_k^*\Big), \quad i = 1, \ldots, 5. \tag{6.5}$$

We expect that β_k will influence the overall values of all I_i^* but will not alter the relative order among the disease prevalence I_i^*. In another word, the highest β_k may not produce the largest I_k^*.

In Fig. 6, the transmission coefficients at each state are given as

$$(\beta_1, \ldots, \beta_5) = (0.2140, 0.1070, 0.3210, 0.4280, 0.2675) \times 10^{-4} \tag{6.6}$$

and plotted in Fig. 6-(b). The disease prevalence at P^* among states is plotted in Fig. 6-(d). We see that the second state has the highest prevalence I_2^*, while it has the lowest transmission coefficient β_2.

Observation II. For transfers among states, the state with the highest in-degree or out-degree may not have the highest disease prevalence.

The impacts of transfer rates δ_{ij} among states on the distribution of I_i^* are highly complex and is an interesting topic worthy of further investigation. In the example shown Fig. 6, the state-transfer network is given in Fig. 6-(a) together with the weights. It is clear from the directed graph that the first state (vertex) has the largest number of edges coming in and going out. Its in-degree and out-degree in the weighted directed graph are both the highest among all states. However, the highest disease prevalence I_i^* occurred at the second state $i = 2$, even when $\alpha_1 = \alpha_2$.

Observation III. Proportions α_i of disease incidence among states have a direct influence on distribution of disease prevalence.

From (6.5) we see that α_i has the direct influence on the number of new infections going into state i. We expect that distribution of I_i^* will mimic that of α_i. As shown in Fig. 6-(c) and Fig. 6-(d), this is indeed the case.

Summarizing our observations, the parameter α_i, which is the proportion of new infections entering the state i, has the most important impact on deciding which state will have the highest disease prevalence. The biological significance of this observation is that it is important for clinical researchers to measure proportions of newly infected HIV patients who are in different HIV states. It is known that some patients whose HIV infection progresses much faster than normal patients, the so-called 'fast progressors', while some patients whose HIV infection progresses much slower, the 'nonprogressors', and others can manage to control the level HIV viral load without treatment treatments, the 'elite controllers' [28,29]. Out results show that it is important for the HIV control to estimate the proportions of these 'abnormal' patients.

6.2. Impacts of transfer among states on the basic reproduction number

The basic reproduction number $\mathcal{R}_0$ determines whether an infectious disease can be effectively controlled. Many disease interventions are aiming at reducing $\mathcal{R}_0$. It can be seen in the expression of $\mathcal{R}_0$ in (4.12) that reducing the transmission coefficients β_i will lower the value of $\mathcal{R}_0$, which is also biologically intuitive. However, the impacts of changing transfer rates among infection states are not so obvious. The transfer rates can be altered through medical interventions. For instance, antiretroviral therapies for HIV infection can decrease and suppress the level of viral load and allow the immune system to recover. This will result in great health benefits for the infected individual. However, if the viral load is not fully suppressed, the infected individual can still be infectious. A healthier condition may allow an individual to resort to riskier sexual behaviours and may make the individual more infectious. While disease amelioration directly benefits an infected individual, its impacts on $\mathcal{R}_0$ and the overall benefits at the community level are far from simple.

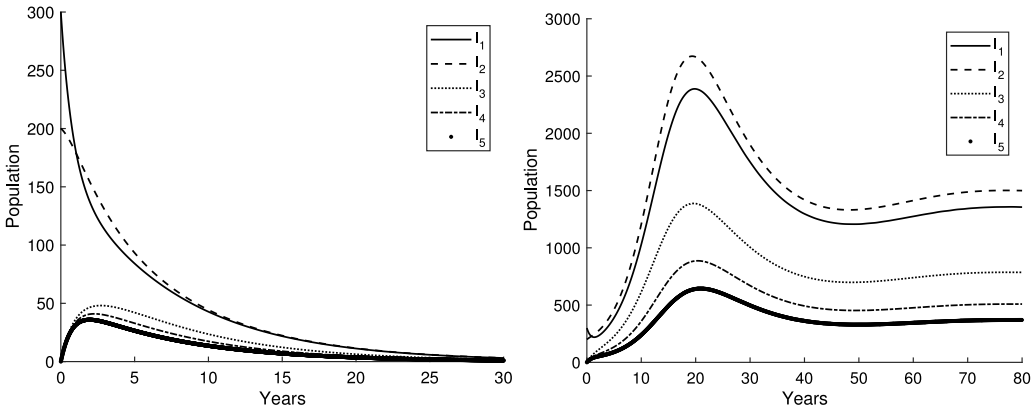

(a) P_0 is globally stable if $\mathcal{R}_0 < 1$. (b) A unique P^* is globally stable if $\mathcal{R}_0 > 1$.

Fig. 5. Simulations for model (6.1) are shown to demonstrate global threshold results in Theorems 5.1 and 5.2. Parameter values are given in (6.2)–(6.4).

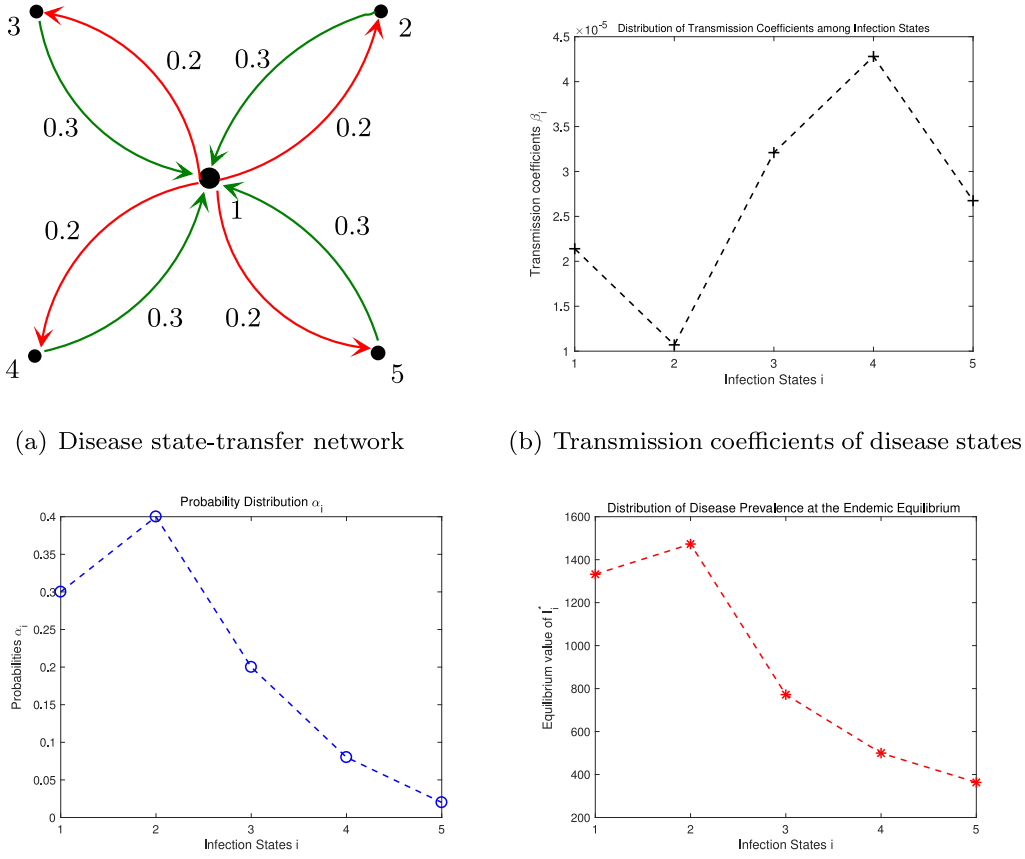

(a) Disease state-transfer network (b) Transmission coefficients of disease states

(c) Proportions of new infections into different states (d) Distribution of infected individuals among states

Fig. 6. Directed graphs for transfers among disease states, transmission coefficients of disease states, fractions of new infections into disease states, and distributions of disease prevalence among states at the endemic equilibrium.

When there are two infected states 1 and 2, when other parameters are fixed in model (6.1), it can be rigorously shown that an increase of δ_{21} or a decrease of δ_{12} can lead to a reduction of $\mathcal{R}_0$ if $R_{01} > R_{02}$, where $R_{0i} = \frac{\beta_i \bar{S}}{\gamma_i + d_i}$, $i = 1, 2$, which are the basic reproduction number of the ith state when it is isolated from other states.

To illustrate the complexity concerning the impacts of state-transfer on basic reproduction number $\mathcal{R}_0$ in model (6.1), we choose the parameters as given in (6.2) and (6.6). Then $R_{01} = 17.12$, $R_{02} = 6.9032$, $R_{03} = 5.8899$, $R_{04} = 5.0353$, $R_{05} = 2.2766$, thus the basic reproduction number $2.2766 \leq \mathcal{R}_0 \leq 17.12$, by (4.12).

Simulation results are shown in Table 1. We can see that an increase in δ_{12}, δ_{31}, δ_{41}, δ_{51} will decease $\mathcal{R}_0$ from its baseline value 6.0074; while an increase of δ_{21}, δ_{13}, δ_{14}, δ_{15} will increase $\mathcal{R}_0$ from the baseline value.

These observations strongly suggest that further theoretical investigations of the impacts of state transfers on the overall dynamics are warranted.

Declaration of competing interest

The authors declare that they have no known competing financial interests or personal relationships that could have appeared to influence the work reported in this paper.

Acknowledgements

The authors wish to thank the anonymous referees whose comments and suggestions have helped to improve the presentation of the manuscript. All authors have participated and approved the final revision.

Appendix

Technical proofs of results in the main sections are provided.

A.1. Proof of Corollary 5.1

We verify relation (5.1). In the following, for two vectors $x = (x_1, \ldots, x_d), y = (y_1, \ldots, y_d) \in \mathbb{R}^d$, relation $x \leq y$ holds if and only if $x_i \leq y_i$ for $i = 1, \ldots, d$. By assumption (H_2), we have $f(N) \leq f(S)$ for all $S \geq 0$. Using assumptions (A_1) and (A_2), we obtain that

$$
\begin{aligned}
(I_1', \ldots, I_n')^T =& \Big(\alpha_1 f(N) \sum_{j=1}^n g_j(S, I_j) + \sum_{j=1}^n \phi_{1j}(I_j) - \psi_1(I_1), \ \ldots, \\
& \qquad \alpha_n f(N) \sum_{j=1}^n g_j(S, I_j) + \sum_{j=1}^n \phi_{nj}(I_j) - \psi_n(I_n) \Big)^T \\
\leq & \Big(\alpha_1 f(\bar{S}) \sum_{j=1}^n g_j(\bar{S}, I_j) + \sum_{j=1}^n \phi_{1j}(I_j) - \psi_1(I_1), \ \cdots, \\
& \qquad \alpha_n f(\bar{S}) \sum_{j=1}^n g_j(\bar{S}, I_j) + \sum_{j=1}^n \phi_{nj}(I_j) - \psi_n(I_n) \Big)^T \\
= & \begin{pmatrix} \frac{\alpha_1 f(\bar{S}) g_1(\bar{S}, I_1)}{I_1} & \cdots & \frac{\alpha_1 f(\bar{S}) g_n(\bar{S}, I_n)}{I_n} \\ \vdots & \ddots & \vdots \\ \frac{\alpha_n f(\bar{S}) g_1(\bar{S}, I_1)}{I_1} & \cdots & \frac{\alpha_n f(\bar{S}) g_n(\bar{S}, I_n)}{I_n} \end{pmatrix} \begin{pmatrix} I_1 \\ \vdots \\ I_n \end{pmatrix} \\
& - \begin{pmatrix} \frac{\psi_1(I_1)}{I_1} & \cdots & -\frac{\phi_{1n}(I_n)}{I_n} \\ \vdots & \ddots & \vdots \\ -\frac{\phi_{n1}(I_1)}{I_1} & \cdots & \frac{\psi_n(I_n)}{I_n} \end{pmatrix} \begin{pmatrix} I_1 \\ \vdots \\ I_n \end{pmatrix} \\
\leq & (F - V)(I_1, \ \ldots, \ I_n)^T.
\end{aligned}
$$

Therefore, condition (5.1) is verified and function L is a Lyapunov function.

A.2. Proof of Proposition 5.2

By Proposition 3.1 and irreducibility of matrix $\bar{M}$, we know that $\tau_i, \bar{\tau} > 0$. Let $(S(t), I_1(t), \ldots, I_n(t))$ be a positive solution of system (4.2) and V be the defined in (5.5). Set $V(t) = V(S(t), I_1(t), \ldots, I_n(t))$. Then

$$
\begin{aligned}
\dot{V} =& \bar{\tau} \Big(1 - \tfrac{\Phi(S^*)}{\Phi(S)} \Big) \Big(\theta(S) - \sum_{j=1}^n g_j(S, I_j) \Big) \\
& + \sum_{i=1}^n \tau_i \Big(1 - \tfrac{\psi_i(I_i^*)}{\psi_i(I_i)} \Big) \Big(\alpha_i \sum_{j=1}^n g_j(S, I_j) + \sum_{j=1}^n \phi_{ij}(I_j) - \psi_i(I_i) \Big).
\end{aligned}
$$

Using equilibrium Eqs. (4.3) we obtain

$$
\begin{aligned}
\dot{V} =& \bar{\tau} \Big(1 - \tfrac{\Phi(S^*)}{\Phi(S)} \Big) \Big(\theta(S) - \theta(S^*) \Big) + \sum_{i=1}^n \tau_i \alpha_i \Big(1 - \tfrac{\Phi(S^*)}{\Phi(S)} \Big) \sum_{j=1}^n g_j(S^*, I_j^*) \\
& + \sum_{i=1}^n \tau_i \alpha_i \Big(\tfrac{\Phi(S^*)}{\Phi(S)} - \tfrac{\psi_i(I_i^*)}{\psi_i(I_i)} \Big) \sum_{j=1}^n g_j(S, I_j) + \sum_{i=1}^n \tau_i \alpha_i \sum_{j=1}^n g_j(S^*, I_j^*) \\
& + \sum_{i=1}^n \tau_i \Big(\sum_{j=1}^n \phi_{ij}(I_j) - \psi_i(I_i) - \sum_{j=1}^n \phi_{ij}(I_j) \tfrac{\psi_i(I_i^*)}{\psi_i(I_i)} + \sum_{j=1}^n \phi_{ij}(I_j^*) \Big) \\
=& \bar{\tau} \Big(1 - \tfrac{\Phi(S^*)}{\Phi(S)} \Big) \Big(\theta(S) - \theta(S^*) \Big) \\
& + \sum_{i=1}^n \tau_i \alpha_i \sum_{j=1}^n g_j(S^*, I_j^*) \Big(2 - \tfrac{\Phi(S^*)}{\Phi(S)} + \tfrac{\Phi(S^*) g_j(S, I_j)}{\Phi(S) g_j(S^*, I_j^*)} - \tfrac{\psi_i(I_i^*) g_j(S, I_j)}{\psi_i(I_i) g_j(S^*, I_j^*)} \Big) \\
& + \sum_{i=1}^n \tau_i \Big(\sum_{j=1}^n \phi_{ij}(I_j) - \tfrac{\psi_i(I_i)}{\psi_i(I_i^*)} \Big(\alpha_i \sum_{j=1}^n g_j(S^*, I_j^*) + \sum_{j=1}^n \phi_{ij}(I_j^*) \Big) \\
& - \sum_{j=1}^n \phi_{ij}(I_j) \tfrac{\psi_i(I_i^*)}{\psi_i(I_i)} + \sum_{j=1}^n \phi_{ij}(I_j^*) \Big) \\
=& \bar{\tau} \Big(1 - \tfrac{\Phi(S^*)}{\Phi(S)} \Big) \Big(\theta(S) - \theta(S^*) \Big) \\
& + \sum_{i=1}^n \tau_i \sum_{j=1}^n \alpha_i g_j(S^*, I_j^*) \Big(2 - \tfrac{\Phi(S^*)}{\Phi(S)} + \tfrac{\Phi(S^*) g_j(S, I_j)}{\Phi(S) g_j(S^*, I_j^*)} \\
& - \tfrac{\psi_i(I_i)}{\psi_i(I_i^*)} - \tfrac{\psi_i(I_i^*) g_j(S, I_j)}{\psi_i(I_i) g_j(S^*, I_j^*)} \Big) \\
& + \sum_{i=1}^n \tau_i \sum_{j=1}^n \phi_{ij}(I_j^*) \Big(1 + \tfrac{\phi_{ij}(I_j)}{\phi_{ij}(I_j^*)} - \tfrac{\psi_i(I_i)}{\psi_i(I_i^*)} - \tfrac{\phi_{ij}(I_j)}{\phi_{ij}(I_j^*)} \tfrac{\psi_i(I_i^*)}{\psi_i(I_i)} \Big).
\end{aligned}
$$

Assumption (B_1) implies that

$$
\Big(1 - \tfrac{\Phi(S^*)}{\Phi(S)} \Big) \Big(\theta(S) - \theta(S^*) \Big) \leq 0.
$$

By assumption (B_3), together with the fact that function $s(x) = 1 - x + \ln x$ has a global maximum at $x = 1$, we obtain

$$
\begin{aligned}
& 1 + \tfrac{\phi_{ij}(I_j)}{\phi_{ij}(I_j^*)} - \tfrac{\psi_i(I_i)}{\psi_i(I_i^*)} - \tfrac{\phi_{ij}(I_j)}{\phi_{ij}(I_j^*)} \tfrac{\psi_i(I_i^*)}{\psi_i(I_i)} \\
&= \Big(\tfrac{\phi_{ij}(I_j)}{\phi_{ij}(I_j^*)} - 1 \Big) \Big(1 - \tfrac{\phi_{ij}(I_j^*)}{\phi_{ij}(I_j)} \tfrac{\psi_j(I_j)}{\psi_j(I_j^*)} \Big) \\
&\quad + \Big(1 - \tfrac{\phi_{ij}(I_j)}{\phi_{ij}(I_j^*)} \tfrac{\psi_i(I_i^*)}{\psi_i(I_i)} + \ln \tfrac{\phi_{ij}(I_j)}{\phi_{ij}(I_j^*)} \tfrac{\psi_i(I_i^*)}{\psi_i(I_i)} \Big) \\
&\quad + \Big(1 - \tfrac{\phi_{ij}(I_j^*)}{\phi_{ij}(I_j)} \tfrac{\psi_j(I_j)}{\psi_j(I_j^*)} + \ln \tfrac{\phi_{ij}(I_j^*)}{\phi_{ij}(I_j)} \tfrac{\psi_j(I_j)}{\psi_j(I_j^*)} \Big) + \tfrac{\psi_j(I_j)}{\psi_j(I_j^*)} \\
&\quad - \ln \tfrac{\psi_j(I_j)}{\psi_j(I_j^*)} - \tfrac{\psi_i(I_i)}{\psi_i(I_i^*)} + \ln \tfrac{\psi_i(I_i)}{\psi_i(I_i^*)} \\
&\leq \tfrac{\psi_j(I_j)}{\psi_j(I_j^*)} - \ln \tfrac{\psi_j(I_j)}{\psi_j(I_j^*)} - \tfrac{\psi_i(I_i)}{\psi_i(I_i^*)} + \ln \tfrac{\psi_i(I_i)}{\psi_i(I_i^*)}.
\end{aligned}
$$

Table 1
Different effects on $\mathcal{R}_0$ of increasing state transfer rates. Up arrows indicate increases from the baseline values and down arrows indicate decreases from the baseline values.

	$(\delta_{21}, \delta_{31}, \delta_{41}, \delta_{51}, \delta_{12}, \delta_{13}, \delta_{14}, \delta_{15})$	$\mathcal{R}_0$
Baseline	(0.2, 0.2, 0.2, 0.2, 0.3, 0.3, 0.3, 0.3)	6.0074
$\delta_{21} \uparrow$	(0.25, 0.2, 0.2, 0.2, 0.3, 0.3, 0.3, 0.3)	6.0216 $\uparrow$
$\delta_{31} \uparrow$	(0.2, 0.25, 0.2, 0.2, 0.3, 0.3, 0.3, 0.3)	6.0009 $\downarrow$
$\delta_{41} \uparrow$	(0.2, 0.2, 0.25, 0.2, 0.3, 0.3, 0.3, 0.3)	5.9568 $\downarrow$
$\delta_{51} \uparrow$	(0.2, 0.2, 0.2, 0.25, 0.3, 0.3, 0.3, 0.3)	5.7936 $\downarrow$
$\delta_{12} \uparrow$	(0.2, 0.2, 0.2, 0.2, 0.35, 0.3, 0.3, 0.3)	5.9931 $\downarrow$
$\delta_{13} \uparrow$	(0.2, 0.2, 0.2, 0.2, 0.3, 0.35, 0.3, 0.3)	6.0110 $\uparrow$
$\delta_{14} \uparrow$	(0.2, 0.2, 0.2, 0.2, 0.3, 0.3, 0.35, 0.3)	6.0265 $\uparrow$
$\delta_{15} \uparrow$	(0.2, 0.2, 0.2, 0.2, 0.3, 0.3, 0.3, 0.35)	6.0674 $\uparrow$

Similarly, using assumption (B_2) we have

$$
\begin{aligned}
&2 - \frac{\Phi(S^*)}{\Phi(S)} + \frac{\Phi(S^*)g_j(S,I_j)}{\Phi(S)g_j(S^*,I_j^*)} - \frac{\psi_i(I_i)}{\psi_i(I_i^*)} - \frac{\psi_i(I_i^*)g_j(S,I_j)}{\psi_i(I_i)g_j(S^*,I_j^*)} \\
&= \left(\frac{\Phi(S^*)g_j(S,I_j)}{\Phi(S)g_j(S^*,I_j^*)} - 1\right)\left(1 - \frac{\Phi(S)\psi_j(I_j)g_j(S^*,I_j^*)}{\Phi(S^*)\psi_j(I_j^*)g_j(S,I_j)}\right) \\
&\quad + \left(1 - \frac{\Phi(S^*)}{\Phi(S)} + \ln\frac{\Phi(S^*)}{\Phi(S)}\right) \\
&\qquad + \left(1 - \frac{\psi_i(I_i^*)g_j(S,I_j)}{\psi_i(I_i)g_j(S^*,I_j^*)} + \ln\frac{\psi_i(I_i^*)g_j(S,I_j)}{\psi_i(I_i)g_j(S^*,I_j^*)}\right) \\
&\qquad + \left(1 - \frac{\Phi(S)\psi_j(I_j)g_j(S^*,I_j^*)}{\Phi(S^*)\psi_j(I_j^*)g_j(S,I_j)} + \ln\frac{\Phi(S)\psi_j(I_j)g_j(S^*,I_j^*)}{\Phi(S^*)\psi_j(I_j^*)g_j(S,I_j)}\right) \\
&\qquad + \frac{\psi_j(I_j)}{\psi_j(I_j^*)} - \ln\frac{\psi_j(I_j)}{\psi_j(I_j^*)} - \frac{\psi_i(I_i)}{\psi_i(I_i^*)} + \ln\frac{\psi_i(I_i)}{\psi_i(I_i^*)} \\
&\le \frac{\psi_j(I_j)}{\psi_j(I_j^*)} - \ln\frac{\psi_j(I_j)}{\psi_j(I_j^*)} - \frac{\psi_i(I_i)}{\psi_i(I_i^*)} + \ln\frac{\psi_i(I_i)}{\psi_i(I_i^*)}.
\end{aligned}
$$

Then, using the definition of $\bar{m}_{ij}$ in (5.4), we obtain

$$
\begin{aligned}
\dot{V} &\le \sum_{i=1}^{n}\tau_i\sum_{j=1}^{n}\alpha_i g_j(S^*,I_j^*)\left(\frac{\psi_j(I_j)}{\psi_j(I_j^*)} - \ln\frac{\psi_j(I_j)}{\psi_j(I_j^*)} - \frac{\psi_i(I_i)}{\psi_i(I_i^*)} + \ln\frac{\psi_i(I_i)}{\psi_i(I_i^*)}\right) \\
&\quad + \sum_{i=1}^{n}\tau_i\sum_{j=1}^{n}\phi_{ij}(I_j^*)\left(\frac{\psi_j(I_j)}{\psi_j(I_j^*)} - \ln\frac{\psi_j(I_j)}{\psi_j(I_j^*)} - \frac{\psi_i(I_i)}{\psi_i(I_i^*)} + \ln\frac{\psi_i(I_i)}{\psi_i(I_i^*)}\right) \\
&= \sum_{i,j=1}^{n}\tau_i\bar{m}_{ij}\left(\frac{\psi_j(I_j)}{\psi_j(I_j^*)} - \ln\frac{\psi_j(I_j)}{\psi_j(I_j^*)} - \frac{\psi_i(I_i)}{\psi_i(I_i^*)} + \ln\frac{\psi_i(I_i)}{\psi_i(I_i^*)}\right).
\end{aligned}
$$

By Propositions 3.2 and 3.3, we have

$$
\sum_{i,j=1}^{n}\tau_i\bar{m}_{ij}\left(\frac{\psi_j(I_j)}{\psi_j(I_j^*)} - \ln\frac{\psi_j(I_j)}{\psi_j(I_j^*)} - \frac{\psi_i(I_i)}{\psi_i(I_i^*)} + \ln\frac{\psi_i(I_i)}{\psi_i(I_i^*)}\right) \equiv 0.
$$

Hence $\dot{V} \le 0$ in the interior of Γ, namely, the function V in (5.5) is a Lyapunov function for system (4.2) in the interior of Γ, completing the proof.

References

[1] W.O. Kermack, A.G. McKendrick, A contribution to the mathematical theory of epidemics, Proc. R. Soc. Lond. Ser. A Math. Phys. Eng. Sci. 115 (772) (1927) 700–721, http://dx.doi.org/10.1098/rspa.1927.0118.

[2] J.A. Jacquez, C.P. Simon, J. Koopman, L. Sattenspiel, T. Perry, Modeling and analyzing HIV transmission: the effect of contact patterns, Math. Biosci. 92 (2) (1988) 119–199, http://dx.doi.org/10.1016/0025-5564(88)90031-4.

[3] H.W. Hethcote, J.W. Van Ark, Modeling HIV transmission and AIDS in the United States, in: Lecture notes in biomathematics, 95, 1991.

[4] J.M. Hyman, J. Li, E.A. Stanley, The differential infectivity and staged progression models for the transmission of HIV, Math. Biosci. 155 (2) (1999) 77–109.

[5] C. McCluskey, A model of HIV/AIDS with staged progression and amelioration, Math. Biosci. 181 (1) (2003) 1–16, http://dx.doi.org/10.1016/s0025-5564(02)00149-9.

[6] A.B. Gumel, C.C. McCluskey, P. van den Driessche, Mathematical study of a staged-progression HIV model with imperfect vaccine, Bull. Math. Biol. 68 (8) (2006) 2105–2128, http://dx.doi.org/10.1007/s11538-006-9095-7.

[7] H. Guo, M.Y. Li, Global dynamics of a staged progression model for infectious diseases, Math. Biosci. Eng. 3 (3) (2006) 513–525, http://dx.doi.org/10.3934/mbe.2006.3.513.

[8] H. Guo, M.Y. Li, Global dynamics of a staged-progression model with amelioration for infectious diseases, J. Biol. Dyn. 2 (2) (2008) 154–168, http://dx.doi.org/10.1080/17513750802120877.

[9] H. Guo, M.Y. Li, Z. Shuai, Global dynamics of a general class of multistage models for infectious diseases, SIAM J. Appl. Math. 72 (1) (2012) 261–279, http://dx.doi.org/10.1137/110827028.

[10] L. Cai, B. Fang, X. Li, A note of a staged progression HIV model with imperfect vaccine, Appl. Math. Comput. 234 (2014) 412–416, http://dx.doi.org/10.1016/j.amc.2014.01.179.

[11] Q. Liu, D. Jiang, Stationary distribution of a stochastic staged progression HIV model with imperfect vaccination, Physica A 527 (2019) 121271, http://dx.doi.org/10.1016/j.physa.2019.121271.

[12] Q. Li, F. Cong, T. Liu, Y. Zhou, Stationary distribution of a stochastic HIV model with two infective stages, Physica A 554 (2020) 124686, http://dx.doi.org/10.1016/j.physa.2020.124686.

[13] O. Diekmann, M. Gyllenberg, J. Metz, H.R. Thieme, The'cumulative'formulation of (physiologically) structured population models, in: Ph. Clement, G. Lumer (Eds.), Evolution Equations, Control Theory, and Biomathematics, Marcel Dekker, 1994, pp. 145–154,, http://dx.doi.org/10.2138/am.2006.1923.

[14] H.R.T. and, Discrete-time population dynamics on the state space of measures, Math. Biosci. Eng. 17 (2) (2020) 1168–1217, http://dx.doi.org/10.3934/mbe.2020061.

[15] W. Jin, H.L. Smith, H.R. Thieme, Persistence versus extinction for a class of discrete-time structured population models, J. Math. Biol. 72 (4) (2015) 821–850, http://dx.doi.org/10.1007/s00285-015-0898-8.

[16] P. Gwiazda, T. Lorenz, A. Marciniak-Czochra, A nonlinear structured population model: Lipschitz continuity of measure-valued solutions with respect to model ingredients, J. Differential Equations 248 (11) (2010) 2703–2735, http://dx.doi.org/10.1016/j.jde.2010.02.010.

[17] V. Dukic, H.F. Lopes, N.G. Polson, Tracking epidemics with google flu trends data and a state-space SEIR model, J. Amer. Statist. Assoc. 107 (500) (2012) 1410–1426, http://dx.doi.org/10.1080/01621459.2012.713876.

[18] K. Genya, S. Shonosuke, T. Hiromasa, O. Takayuki, Predicting intervention effect for COVID-19 in Japan: state space modeling approach., BioSci. Trends 14 (3) (2020) 174–181.

[19] F.M. Bass, A new product growth for model consumer durables, Manage. Sci. 15 (5) (1969) 215–227.

[20] A. Mellor, M. Mobilia, S. Redner, A.M. Rucklidge, J.A. Ward, Influence of luddism on innovation diffusion, Phys. Rev. E 92 (1) (2015) http://dx.doi.org/10.1103/physreve.92.012806.

[21] S. Moldovan, J. Goldenberg, Cellular automata modeling of resistance to innovations: Effects and solutions, Technol. Forecast. Soc. Change 71 (5) (2004) 425–442, http://dx.doi.org/10.1016/s0040-1625(03)00026-x.

[22] F. Xiong, Y. Liu, Z. jiang Zhang, J. Zhu, Y. Zhang, An information diffusion model based on retweeting mechanism for online social media, Phys. Lett. A 376 (30–31) (2012) 2103–2108, http://dx.doi.org/10.1016/j.physleta.2012.05.021.

[23] D. Stauffer, M. Sahimi, Can a few fanatics influence the opinion of a large segment of a society? Eur. Phys. J. B 57 (2) (2007) 147–152, http://dx.doi.org/10.1140/epjb/e2007-00106-7.

[24] P.L. Krapivsky, S. Redner, D. Volovik, Reinforcement-driven spread of innovations and fads, J. Stat. Mech. Theory Exp. 2011 (12) (2011) P12003, http://dx.doi.org/10.1088/1742-5468/2011/12/p12003.

[25] G.F. de Arruda, F.A. Rodrigues, P.M. Rodríguez, E. Cozzo, Y. Moreno, A general Markov chain approach for disease and rumour spreading in complex networks, J. Complex Netw. 6 (2) (2017) 215–242, http://dx.doi.org/10.1093/comnet/cnx024.

[26] C. Kyriakopoulos, G. Grossmann, V. Wolf, L. Bortolussi, Lumping of degree-based mean-field and pair-approximation equations for multistate contact processes, Phys. Rev. E 97 (1) (2018) http://dx.doi.org/10.1103/physreve.97.012301.

[27] C. Kaligotla, E. Yücesan, S.E. Chick, Diffusion of competing rumours on social media, J. Simulat. (2020) 1–21, http://dx.doi.org/10.1080/17477778.2020.1785345.

[28] O. Lambotte, G. Ferrari, C. Moog, N.L. Yates, H.-X. Liao, R.J. Parks, C.B. Hicks, K. Owzar, G.D. Tomaras, D.C. Montefiori, B.F. Haynes, J.-F. Delfraissy, Heterogeneous neutralizing antibody and antibody-dependent cell cytotoxicity responses in HIV-1 elite controllers, AIDS 23 (8) (2009) 897–906, http://dx.doi.org/10.1097/qad.0b013e328329f97d.

[29] J.F. Okulicz, O. Lambotte, Epidemiology and clinical characteristics of elite controllers, Curr. Opin. HIV AIDS 6 (3) (2011) 163–168, http://dx.doi.org/10.1097/coh.0b013e328344f35e.

[30] S.M. Goodreau, E.S. Rosenberg, S.M. Jenness, N. Luisi, S.E. Stansfield, G.A. Millett, P.S. Sullivan, Sources of racial disparities in HIV prevalence in men who have sex with men in atlanta, GA, USA: a modelling study, The Lancet HIV 4 (7) (2017) e311–e320, http://dx.doi.org/10.1016/s2352-3018(17)30067-x.
[31] D. Hansson, K. Leung, T. Britton, S. Strömdahl, A dynamic network model to disentangle the roles of steady and casual partners for HIV transmission among MSM, Epidemics 27 (2019) 66–76, http://dx.doi.org/10.1016/j.epidem.2019.02.001.
[32] R. Li, S. Pei, B. Chen, Y. Song, T. Zhang, W. Yang, J. Shaman, Substantial undocumented infection facilitates the rapid dissemination of novel coronavirus (SARS-CoV2), Science 368 (6490) (2020) 489–493, http://dx.doi.org/10.1126/science.abb3221.
[33] M. Gandhi, D.S. Yokoe, D.V. Havlir, Asymptomatic transmission, the achilles' heel of current strategies to control Covid-19, New Engl. J. Med. 382 (22) (2020) 2158–2160, http://dx.doi.org/10.1056/NEJMe2009758.
[34] M. Lipsitch, N.E. Dean, Understanding COVID-19 vaccine efficacy, Science 370 (6518) (2020) 763–765, http://dx.doi.org/10.1126/science.abe5938, URL https://science.sciencemag.org/content/370/6518/763.
[35] D. Kalajdzievska, M.Y. Li, Modeling the effects of carriers on transmission dynamics of infectious diseases, Math. Biosci. Eng 8 (2011) 711–722.
[36] M. Cadoni, G. Gaeta, Size and timescale of epidemics in the SIR framework, Physica D 411 (2020) 132626, http://dx.doi.org/10.1016/j.physd.2020.132626, URL https://www.sciencedirect.com/science/article/pii/S0167278920302803.
[37] G. Gaeta, A simple SIR model with a large set of asymptomatic infectives, Math. Eng. 3 (2021) 1–39, http://dx.doi.org/10.3934/mine.2021013.
[38] A. Ramos, M. Ferrández, M. Vela-Pérez, A. Kubik, B. Ivorra, A simple but complex enough θ-SIR type model to be used with COVID-19 real data. Application to the case of Italy, Physica D (2021) 132839, http://dx.doi.org/10.1016/j.physd.2020.132839.
[39] C. Vyasarayani, A. Chatterjee, New approximations, and policy implications, from a delayed dynamic model of a fast pandemic, Physica D 414 (2020) 132701, http://dx.doi.org/10.1016/j.physd.2020.132701.
[40] P.J. Hurtado, A.S. Kirosingh, Generalizations of the 'linear chain trick': incorporating more flexible dwell time distributions into mean field ODE models, J. Math. Biol. 79 (5) (2019) 1831–1883, http://dx.doi.org/10.1007/s00285-019-01412-w.
[41] J.P. Gleeson, Binary-state dynamics on complex networks: Pair approximation and beyond, Phys. Rev. X 3 (2) (2013) http://dx.doi.org/10.1103/physrevx.3.021004.
[42] P.G. Fennell, J.P. Gleeson, Multistate dynamical processes on networks: Analysis through degree-based approximation frameworks, SIAM Rev. 61 (1) (2019) 92–118, http://dx.doi.org/10.1137/16m1109345.
[43] H. Guo, M. Li, Z. Shuai, A graph-theoretic approach to the method of global Lyapunov functions, Proc. Amer. Math. Soc. 136 (8) (2008) 2793–2802.
[44] M.Y. Li, Z. Shuai, Global-stability problem for coupled systems of differential equations on networks, J. Differential Equations 248 (1) (2010) 1–20.
[45] Z. Qiu, M.Y. Li, Z. Shen, Global dynamics of an infinite dimensional epidemic model with nonlocal state structures, J. Differential Equations 265 (10) (2018) 5262–5296, http://dx.doi.org/10.1016/j.jde.2018.06.036.
[46] H. Guo, M.Y. Li, Global dynamics of a staged-progression model for HIV/AIDS with amelioration, Nonlinear Anal. RWA 12 (5) (2011) 2529–2540, http://dx.doi.org/10.1016/j.nonrwa.2011.02.021.
[47] F. Nyabadza, Z. Mukandavire, S. Hove-Musekwa, Modelling the HIV/AIDS epidemic trends in South Africa: Insights from a simple mathematical model, Nonlinear Anal. RWA 12 (4) (2011) 2091–2104, http://dx.doi.org/10.1016/j.nonrwa.2010.12.024.
[48] T. Viljoen, J. Spoelstra, L. Hemerik, J. Molenaar, Modelling the impact of HIV on the populations of South Africa and botswana, Acta Biotheor. 62 (1) (2014) 91–108, http://dx.doi.org/10.1007/s10441-014-9210-3.
[49] R. de Boer, M.Y. Li, Density dependence in disease incidence and its impacts on transmission dynamics, Can. Appl. Math. Q. 19 (3) (2012) 195–218.
[50] A. Berman, R.J. Plemmons, Nonnegative Matrices in the Mathematical Sciences, SIAM, 1994.
[51] J. Moon, Counting Labelled Trees, William Clowes and Sons, London, 1970.
[52] G. Kirchhoff, Ueber die Auflösung der Gleichungen, auf welche man bei der Untersuchung der linearen Vertheilung galvanischer Ströme geführt wird, Ann. Phys. Chem. 148 (12) (1847) 497–508, http://dx.doi.org/10.1002/andp.18471481202.
[53] J. Maidens, M.Y. Li, Global Lyapunov functions and a hierarchical control scheme for networks of robotic agents, in: 2013 American Control Conference, IEEE, 2013, http://dx.doi.org/10.1109/acc.2013.6580460.
[54] J. Arino, Diseases in metapopulations, in: Modeling and Dynamics of Infectious Diseases, World Scientific, 2009, pp. 64–122, http://dx.doi.org/10.1142/9789814261265_0003.
[55] P. Du, M.Y. Li, Impact of network connectivity on the synchronization and global dynamics of coupled systems of differential equations, Physica D 286–287 (2014) 32–42, http://dx.doi.org/10.1016/j.physd.2014.07.008.
[56] O. Diekmann, J.A.P. Heesterbeek, J.A. Metz, On the definition and the computation of the basic reproduction ratio R0 in models for infectious diseases in heterogeneous populations, J. Math. Biol. 28 (4) (1990) 365–382.
[57] P.V. den Driessche, J. Watmough, Reproduction numbers and sub-threshold endemic equilibria for compartmental models of disease transmission, Math. Biosci. 180 (1) (2002) 29–48.
[58] Z. Feng, Final and peak epidemic sizes for SEIR models with quarantine and isolation., Math. Biosci. Eng.: MBE 4 (4) (2007) 675–686.
[59] H. Song, S. Liu, W. Jiang, Global dynamics of a multistage SIR model with distributed delays and nonlinear incidence rate, Math. Methods Appl. Sci. 40 (6) (2017) 2153–2164.
[60] J.P. La Salle, The Stability of Dynamical Systems, SIAM, 1976.
[61] H. Freedman, S. Ruan, M. Tang, Uniform persistence and flows near a closed positively invariant set, J. Dynam. Differential Equations 6 (4) (1994) 583–600.
[62] M.Y. Li, J.R. Graef, L. Wang, J. Karsai, Global dynamics of a SEIR model with varying total population size, Math. Biosci. 160 (2) (1999) 191–213.
[63] H.L. Smith, P. Waltman, The Theory of the Chemostat: Dynamics of Microbial Competition, 13, Cambridge university press, 1995.
[64] N.P. Bhatia, G.P. Szegö, Dynamical Systems: Stability Theory and Applications, Springer, 1967.
[65] Z. Su, C. Dong, P. Li, H. Deng, Y. Gong, S. Zhong, M. Wu, Y. Ruan, G. Qin, W. Yang, Y. Shao, M. Li, A mathematical modeling study of the HIV epidemics at two rural townships in the liangshan prefecture of the sichuan province of China, Infect. Dis. Model. 1 (1) (2016) 3–10, http://dx.doi.org/10.1016/j.idm.2016.05.001.